DEVELOPMENT OF Ni AND NiO BASED ELECTROCATALYTIC MATERIAL TO SYNTHESIZE POLLUTION FREE RENEWABLE ENERGY BY ELECTROOXIDATION OF GLUCOSE BASED FUEL

Thesis Submitted in Partial Fulfillment of the

Requirements for the Degree of

Master of Technology in Material Engineering

BY

Amit Kumar Mondal

[Examination Roll No: M4MAT19023]

[University Registration No: 140914 of 2017-2018]

UNDER THE GUIDANCE OF

PROF. SUBIR PAUL

DEPARTMENT OF METALLURGICAL AND MATERIAL ENGINEERING

FACULTY OF ENGINEERING & TECHNOLOGY

JADAVPUR UNIVERSITY

KOLKATA – 700032

MAY 2019

FACULTY OF ENGINEERING AND TECHNOLOGY

JADAVPUR UNIVERSITY

CERTIFICATE OF APPROVAL*

This foregoing thesis is hereby approved as a credible study of an engineering subject carried out and presented in a manner satisfactory to warrant its acceptance as a prerequisite to the degree for which it has been submitted. It is understood that by this approval the undersigned do not endorse or approve any statement made, opinion expressed or conclusion drawn therein but approve the thesis only for the purpose for which it has been submitted.

COMMITTEE ----------

ON FINAL EXAMINATION FOR

EVALUATION OF THE THESIS ----------

***Only in case the thesis is approved**

JADAVPUR UNIVERSITY

FACULTY OF ENGINEERING AND TECHNOLOGY

Certificate of Recommendation

This is to certify that the entitled '*DEVELOPMENT OF Ni AND NiO BASED ELECCTROCATALYTIC MATERIAL TO SYNTHESIZE POLLUTION FREE RENEWABLE ENERGY BY ELECTROOXIDATION OF GLUCOSE BASED FUEL'* has been carried out by Mr. Amit Kumar Mondal *(Examination Roll No: M4MAT19023 , Registration No: 140914 of 2017-2018)* under my guidance and supervision and accepted in partial fulfilment for the degree of Master of Technology in Material Engineering from Jadavpur University. To the best of our knowledge the contents of this thesis or any part thereof have not been previously submitted for the award of any degree or diploma.

……..

Prof. Subir Paul
Professor,
Department of Metallurgical & Material Engineering
Jadavpur University
Kolkata-700032

……

Prof. Chiranjib Bhattacharjee
Dean,
Faculty of Engineering and Technology
Jadavpur University
Kolkata-700032

……

Prof. A.K. Pramanick
Head of the Department,
Department of Metallurgical & Material Engineering
Jadavpur University
Kolkata-700032

DECLARATION OF ORIGINALITY AND COMPLIANCE OF ACADEMIC ETHICS

I hereby declare that the thesis contains literature survey and original research work by the undersigned candidate, as a part of his *MASTER OF TECHNOLOGY IN MATERIAL ENGINEERING* studies. All information in this document have been obtained and presented in accordance with the academic rules and ethical conduct.

I also declare that, as required by these rules of conduct, I have fully cited and referenced all the material and results that are not original to this work.

Name: AMIT KUMAR MONDAL

Examination Roll Number: M4MAT19023

Class Roll Number: 001711303024

University Registration No: 140914 of 2017-18

Thesis Title: *DEVELOPMENT OF Ni AND NiO BASED ELECTROCATALYTIC MATERIAL TO SYNTHESIZE POLLUTION FREE RENEWABLE ENERGY BY ELECTROOXIDATION OF GLUCOSE BASED FUEL.*

Signature with Date:

ACKNOWLEDGEMENT

I would like to offer my sincere thanks to all who provided me this opportunity and granted me the capability to proceed successfully with my thesis. This thesis appears in its current form due to the assistance and guidance of several people.

I express my deep sense of gratitude to my supervisor, Dr. Subir Paul, Professor, Department of Metallurgical and Material Engineering, Jadavpur University, for his inspiration, support, academic and personal guidance throughout the course work. I'm grateful to him for being very supportive in letting me pursue my interests outside of academics, and encouraging me to learn and read widely. I'm grateful for this opportunity and look forward to continue my interactions with him in future.

I'm very fortunate to be a part of the Electrochemistry and Corrosion Lab, Jadavpur University and my thanks also goes to all lab assistants for providing excellent working experience.

My thanks also goes to all my batch mates who have made the atmosphere in my classes lively. This work would not have been successful without the support and suggestions of respected professors of Metallurgical and Material Engineering Department, Jadavpur University. The excellent cooperation and support by research scholars are thankfully acknowledged.

Last, but most importantly, I'm grateful to my parents and family for their love, blessings and support throughout this endeavor. This thesis, a fruit of the combined efforts of my family members, is dedicated to them as a token of love and gratitude.

Date: May 2019 (Amit Kumar Mondal)

Contents

Chapter 1 :Introduction

Chapter1: Introduction

Automobile and transportation on land and in air are the major causes of global environment pollution through the chemical combustion of petroleum fuels. To meet the challenge of rising demand for energy, at the same time, reducing environmental pollution, the energy synthesis through electrochemical oxidation of fuels, in fuel cell is a promising alternative green energy technology. Pure electrical energy in fuel cell through electro oxidation of various renewable fuels over high energetic electrocatalytic substrate is an innovative solution to meet the challenge.

Glucose is a good green renewable fuel, abundantly available in cane sugar and agricultural waste. The electrochemical oxidation of glucose fuel can produce as high as 1.35KJ/gm of energy.

Development of fuel cell lies on exhaustive research on development of high energetic electro catalytic electrodes over which the fuel breaks down to produce free electron and ions, delivering electrical energy. The present work aims at developing two electrocatalytic materials Ni and Ni-NiO by electro synthesis method. Graphene was also codeposited on Ni-NiO to enhance the electrocatalytic property of the material.

The performance of the materials was investigated by Electrochemical characterization viz. Cyclic voltammetry (CV), Chronoammetry (CA) and Potentiodynamic Polarization (PD). Electrochemical properties, reversible cell potential and current were computed.

To investigate further, the electrochemical phenomenon occurring at electrode-solution interface, Electrochemical Impedance Spectroscopy (EIS) studies were performed. Polarization resistance, Impedance and double layer capacitance were computed. The R-L-C circuit evaluated from EIS studies helped to understand the fundamental science of find high energetic material on glucose oxidation by Ni and NiO coatings.

The constituents and phases of the electrode materials as analyzed by XRD and the morphology of the 3D structure studied by SEM, helped to understand fundamental science behind high electrochemical current from glucose oxidation.

The present investigation is route to find a novel way of synthesizing clean and green energy using glucose-based agriculture crops and waste. The materials were found to deliver a high current on electro oxidation of glucose.

Chapter 2:

Literature Review

Chapter 2: Literature Review

Since the present work is aimed to the development of electrode for fuel cell, a survey on available literatures on both Fuel cell, Fuel cell systems and Fuel cell electrodes and catalytic surfaces. As the energy conversion from fuel to electrical energy occurs at the catalytic surfaces of the electrodes it is necessary to characterize them electrochemically and morphologically, an effort has been made to survey the available literatures on electrochemical and morphological characterization techniques performed regarding the presented work. Therefore, in the following section the literature review is presented.

2.1 Fuel Cell:

A fuel cell is an electrochemical energy producing device that converts stored chemical potential energy in the molecular bonds of fuels into pure electrical energy through a pair of redox reactions.

The history of fuel cells goes back to 1838 when Welsh physicist William Robert Grove and German-Swiss chemist Christian Friedreich Schönbein developed their first set of crude Fuel cells quite simultaneously.

2.1.1 Working principle:

A fuel cell as described is basically a electrochemical cell are consisting of three adjacent segments namely -two electrodes -an anode, a cathode and an electrolyte. On contrary to conventional battery also an electrochemical cell producing electrical energy where one of the electrodes is sacrificial (except flow batteries where Reversible reactions restores the cell components during recharging of the battery) , the fuel cell electrodes are not sacrificial , instead they requires a steady supply of fuels and an oxidizing agent (usually oxygen from air) to sustain the cell reactions. The electrodes contain catalytic surfaces those are separated by a specific ion conducting membrane or an electrolyte. At anode a electrochemical reaction triggers the fuel to undergo an oxidation on the catalytic surface leading to the generation of an ion (often an positive hydrogen ion or proton) which then

moves to the cathode catalytic surface through the electrolyte medium within the cell. In the meaning time electrons generated in the anode reaction travels to the cathode through an external load to the cathode. Now the electrons, the ions travelled through the electrolyte and oxygen reacts on the cathode catalytic surface to generate water and if possible, some other products. Single fuel cell often produces very low voltage often in the order of 0.7V. So according to application requirement individual cells are stacked alternatively to ramp up the voltage.

2.1.2 Types of Fuel cell:

Since their earlier days fuel cells have come a long way and have emerged into different varieties according to their development. Depending on the design features of the fuel cell from the aspect of the electrolyte used that generally defines the fuel cell type, the fuel used, catalyst material on anode, catalyst material used in cathode, oxidization resisted gas diffusion layers fuel cells can be categorized in the following way:

2.2.2 Alkaline Fuel Cell (AFC):

Alkaline Fuel Cell first successfully developed by English Engineer Francis Thomas Beckon and demonstrated in 1959 to public was the first hydrogen -oxygen based fuel cell which used aqueous potassium hydroxide (KOH) as electrolyte. AFCs uses suitable catalysts like Pt, Ag, CoO impregnated on porous carbon matrix or LiOH soaked and dried porous NiO matrix as electrodes and a matrix saturated with aqueous KOH or NaOH acts as an electrolyte medium. The redox reactions for fuel cells power production is given by the following:

At anode hydrogen gas is oxidized to produce water and electron: $H_2 + 2OH^- \rightarrow 2H_2O + 2e^-$

Electrons travel to cathode via external circuit to reduce oxygen given by the reaction: $O_2 + H_2O + 4e^- \rightarrow 4OH^-$

The aqueous KOH electrolyte pose a threat to the AFCs because it combines with CO_2 to produce K_2CO_3 which reduces the conductivity of the electrolyte and decreasing cell efficiency. It can also deteriorate the catalytic surfaces. So AFCs should always work under pure oxygen environment.

The subtype alkaline fuel cell is Alkaline Anion Exchange Membrane Fuel Cell (AAEMFC). They are also referred as Anion Exchange Membrane Fuel Cell (AEMFC) or Alkaline Membrane Fuel Cell (AMFC). They use polymer membrane instead of aqueous potassium hydroxide as an electrolyte.

2.2.3 Proton Exchange Membrane Fuel Cells (PEMFCs) :

Proton Exchange Membrane Fuel Cells are solid polymer electrolyte fuel cells in which the solid polymer (NAFION) is the electrolyte and it uses hydrogen and oxygen as fuel. On the anode hydrogen gas diffuses in the catalyst and later dissociates into an electron and a proton. These protons are conducted through the polymer membrane to the cathode catalyst to react with the oxygen and to produce water. As the membranes only allow protons to pass through the electrons produced in anode are forced to travel via external circuit to the cathode. At anode :

$$H_2 \rightarrow 2H^+ + 2e^- \qquad E^0 = 0V \qquad \frac{dE^0}{dT} = 0mVK^{-1}$$

At cathode :

$$H_2 + \frac{1}{2}O_2 \rightarrow H_2O \qquad E^0 = 1.2291V \qquad \frac{dE^0}{dT} = -0.8456\,mV\,K^{-1}$$

Overall reaction :

$$H_2 + \frac{1}{2}O_2 \rightarrow H_2O \qquad E_0 = 1.2291V \qquad \frac{dE_0}{dT} = -0.8456\,mV\,K^{-1}$$

2.2.4 Phosphoric Acid Fuel Cell:

Phosphoric acid fuel cells (PAFC) are first commercialized fuel cells. They use finely dispersed catalyst coated carbon catalyst as electrodes and silicon carbide matrix

saturated in highly concentrated or pure liquid phosphoric acid. Operating Temperature of the PAFC are in the range of 150 ºC to 250 ºC.

2.2.5 Solid Acid Fuel Cell:

Solid acid Fuel Cells first developed by Sossina M. Haile, an Ethiopian-American chemist in 1990's uses as its name suggests solid acid material as electrolyte medium. It generates electricity by electrochemical reactions of hydrogen and oxygen containing gases by producing water as byproduct.

Solid acids often used as heterogeneous catalysts do not dissolve in the reaction medium. They are intermediate between salts and acids. Though $CsHSO_4$ is mainly used as electrolyte it has been shown that $CsHSeO_4$, $Rb_3H(SeO_4)_2$, $(NH_4)_3H(SO_4)_2$; $K_3H(SO_4)_2$ can be used as the electrolyte system of solid acid. The operating temperature of the solid acid fuel cell varies in between 200ºC to 300 ºC. The electrode reactions are as follows:

$$Anode: H_2 \rightarrow 2H^+ + 2e^-$$

$$Cathode: \frac{1}{2}O_2 + 2H^+ + 2e^- \rightarrow H_2O$$

$$Overall: H_2 + \frac{1}{2}O_2 \rightarrow H_2O$$

The solid acid conductivity, the driving factor for the SAFC performance and efficiency depends upon the temperature of the fuel cell and at a certain temperature super protonic transition of the solid acid occurs.

2.2.6 High Temperature Fuel Cell:

High temperature fuel cells are those which operate above 500 ºC temperature and a range of 500 ºC to 1000 ºC They are mainly of two types, namely- solid oxide fuel cell and molten carbonate fuel cell.

2.2.6.1 Solid Oxide Fuel Cell:

Solid oxide fuel cells are characterized by the use of ceramic type solid oxide electrolytes which are activated as conducting medium at a certain higher temperature with significant amount of conductivity. The general operating temperature though varies between 800ºC to 1000ºC .

In solid oxide fuel cell the fuel generally used is either hydrogen or carbon monooxide. The solid electrolytes conduct negative oxygen ions from cathode to anode. Electrochemical oxidation of the oxygen ions occurs with the fuel on the anode side of the electrode. SOFCs are advantageous to the point that these do not require costly platinum catalysts as electrode thus making them cheaper than low temperature PEMFCs. Though SOFC electrodes are not prone to carbon monoxide poisoning but they are sensitiveness to sulfur poisoning has been widely observed and hence the fuel must be removed of sulfur before entering the cell by use of Sulphur adsorbent bed or other appropriate methods.

A SOFC is made up of four layers, out of which three are ceramics namely anode, cathode ,and electrolyte and a fourth layer of interconnection. The SOFC stack can be of planar type or microtubular type. The problem of thermal expansion requires a uniform and well regulated heating process for starting up. The start up time for planar stack sofc is on the order of an hour but in case of the microtubular stack it is in the order of minutes.

The ceramic anode layer must be very porous to allow the fuel to flow towards the electrolyte. Consequently, granular matter is often selected for anode fabrication procedures. Like the cathode, it must conduct electrons, with ionic conductivity a definite asset. The most common material used is a cermet made up of nickel mixed with the ceramic material that is used for the electrolyte in that particular cell, typically YSZ (yttria stabilized zirconia) nanomaterial-based catalysts, this YSZ part helps stop the grain growth of nickel. Larger grains of nickel would reduce the contact area that ions can be conducted through, which would lower the cells efficiency. The anode is commonly the thickest and strongest layer in each individual cell, because it has the smallest polarization losses, and is often the layer that provides the mechanical support. Electrochemically speaking, the anode’s job is to use the oxygen ions that diffuse through the electrolyte to oxidize the hydrogen fuel. The oxidation reaction between the oxygen ions and the hydrogen produces heat as well as water and electricity. If the fuel is a light hydrocarbon, for example, methane, another function of the anode is to act as a catalyst for steam reforming the fuel into

hydrogen. This provides another operational benefit to the fuel cell stack because the reforming reaction is endothermic, which cools the stack internally. Perovskite materials (mixed ionic/electronic conducting ceramics) have been shown to produce a power density of 0.6 W/cm^2 at 0.7 V at 800 °C which is possible because they have the ability to overcome a larger activation energy.

The electrolyte is a dense layer of ceramic that conducts oxygen ions. Its electronic conductivity must be kept as low as possible to prevent losses from leakage currents. The high operating temperatures of SOFCs allow the kinetics of oxygen ion transport to be sufficient for good performance. However, as the operating temperature approaches the lower limit for SOFCs at around 600 °C, the electrolyte begins to have large ionic transport resistances and affect the performance. Popular electrolyte materials include yttria-stabilized zirconia (YSZ) (often the 8% form 8YSZ), scandia stabilized zirconia (ScSZ) (usually 9 mol% Sc_2O_3– 9ScSZ) and gadolinium doped ceria (GDC) The electrolyte material has crucial influence on the cell performances. Detrimental reactions between YSZ electrolytes and modern cathodes such as lanthanum strontium cobalt ferrite (LSCF) have been found, and can be prevented by thin (<100 nm) ceria diffusion barriers.

The cathode, or air electrode, is a thin porous layer on the electrolyte where oxygen reduction takes place. The overall reaction is written in Kröger-Vink Notation as follows:

$$\frac{1}{2}O_2(g) + 2e' + V_o^{\bullet\bullet} \rightarrow O_o^{\times}$$

Cathode materials must be, at a minimum, electronically conductive. Currently, lanthanum strontium manganite (LSM) is the cathode material of choice for commercial use because of its compatibility with doped zirconia electrolytes. Mechanically, it has a similar coefficient of thermal expansion to YSZ and thus limits stress buildup because of CTE mismatch. Also, LSM has low levels of chemical reactivity with YSZ which extends the lifetime of the materials. Unfortunately, LSM is a poor ionic conductor, and so the electrochemically active reaction is limited to the triple phase boundary (TPB) where the electrolyte, air and electrode meet. LSM works well as a cathode at high temperatures, but its performance quickly falls as the operating temperature is lowered below 800 °C. In order to increase the reaction zone beyond the TPB, a potential cathode material must be able to conduct both electrons and oxygen ions. Composite cathodes consisting of LSM YSZ have

been used to increase this triple phase boundary length. Mixed ionic/electronic conducting (MIEC) ceramics, such as perovskite LSCF, are also being researched for use in intermediate temperature SOFCs as they are more active and can make up for the increase in the activation energy of the reaction.

The interconnect can be either a metallic or ceramic layer that sits between each individual cell. Its purpose is to connect each cell in series, so that the electricity each cell generates can be combined. Because the interconnect is exposed to both the oxidizing and reducing side of the cell at high temperatures, it must be extremely stable. For this reason, ceramics have been more successful in the long term than metals as interconnect materials. However, these ceramic interconnect materials are very expensive as compared to metals. Nickel- and steel-based alloys are becoming more promising as lower temperature (600–800 °C) SOFCs are developed. The material of choice for an interconnect in contact with Y8SZ is a metallic 95Cr-5Fe alloy. Ceramic-metal composites called 'cermet' are also under consideration, as they have demonstrated thermal stability at high temperatures and excellent electrical conductivity.

2.2.6.2 Molten Carbonate Fuel Cell

Molten carbonate fuel cells are the second type of high temperature fuel cells operating at a temp of 600 ºC and above and uses molten carbonate salts in the liquid electrolyte form which consists of sodium and potassium in a lithium aluminate($LiAlO_2$) porous matrix.

The anode material consists of porous Ni based alloy often alloyed with Chromium or Aluminium. The cathode material is composed of porous Ni later converted to lithiated nickel oxide by intercalation within the NiO crystal structure.

Unlike alkaline, phosphoric acid, and polymer electrolyte membrane fuel cells, MCFCs don't require an external reformer to convert more energy-dense fuels to hydrogen. Due to the high temperatures at which MCFCs operate, these fuels are converted to

hydrogen within the fuel cell itself by a process called internal reforming, which also reduces cost.

Molten carbonate fuel cells are not prone to poisoning by carbon monoxide or carbon dioxide — they can even use carbon oxides as fuel — making them more attractive for fueling with gases made from coal. Because they are more resistant to impurities than other fuel cell types, scientists believe that they could even be capable of internal reforming of coal, assuming they can be made resistant to impurities such as sulfur and particulates that result from converting coal, a dirtier fossil fuel source than many others, into hydrogen. Alternatively, because MCFCs require CO_2 be delivered to the cathode along with the oxidizer, they can be used to electrochemically separate carbon dioxide from the flue gas of other fossil fuel power plants for sequestration.

Due to the production of CO_2 during reforming of the fossil fuel (methane, natural gas), MCFCs are not a completely green technology, but are promising due to their reliability and efficiency (sufficient heat for co-generation with electricity). Current MCFC efficiencies range from 60-70%. Reactions:

$$Internal\ \ Reformer: \quad CH_4 + H_2O = 3H_2 + CO$$

$$Anode: \qquad H_2 + CO_3^{=} = H_2O + CO_2 + 2e^-$$

$$Cathode: \qquad \frac{1}{2}O_2 + CO_2 + 2e^- = CO_3^{=}$$

$$Cell: \quad H_2 + \frac{1}{2}O_2 = H_2O$$

$$Nernst\ \ Equation: \qquad E = E^o + \frac{RT}{2F} log \frac{P_{H_2} P_{O_2}^{\frac{1}{2}}}{P_{H_2O}} + \frac{RT}{2F} log \frac{P_{CO_2,cathode}}{P_{CO_2,anode}}$$

2.2.7 Direct Methanol fuel Cell

Direct methanol fuel cells, a subcategory of proton-exchange fuel cells uses methanol as fuel. Though its efficiency is very low, it is targeted to be used especially in portable applications where energy and power density are of primary interest.

Where indirect methanol uses the hydrogen, produced from methanol by steam reforming , the direct methanol fuel cell uses methanol solution to carry the reactant into

the cell. The DMFC relies upon the oxidation of methanol on a catalyst layer to form carbon dioxide. Water is consumed at anode and produced at cathode. Proton transportation occurs across proton exchange membrane often made of nafion to the cathode. In cathode protons react with oxygen to produce water. The half cell reactions can be given by:

$$\textit{Anode oxidation}: \quad CH_3OH + H_2O \rightarrow 6\,H^+ + 6\,e^- + CO_2$$

$$\textit{Cathode reduction}: \frac{3}{2}O_2 + 6\,H^+ + 6\,e^- \rightarrow 3\,H_2O$$

$$\textit{Overall redox reaction}: CH_3OH + \frac{3}{2}O_2 \rightarrow 2\,H_2O + CO_2$$

2.2.8 Direct ethanol Fuel Cell:

Direct ethanol fuel cells works in the same principle of direct methanol fuel cell ,except the fuel used here is ethanol , non-toxic on the contrary to methanol and an existing production method is in place for development of fuel. They mainly categorize under PEMFC according to working principle but the direct oxidation of the ethanol occurs at high performance nanostructured electrodes made of Ni-Co-Fe base are cheaper than noble electrocatalytic material like platinum grade anode .Pure Ni based cathode electrode has been reported to be used.

Water is consumed at anode to oxidize ethanol to produce hydrogen ion, electron and carbon-di-oxide. The electrons travel through external circuit to the cathode and gives of electrical energy. Meanwhile the hydrogen atom is transported through the polymer electrolytic membrane to the cathode side to react with the cathode side electron and oxygen to produce water. The reactions are given by as follows:

$$\textit{Anode}: \quad C_2H_5OH + H_2O \rightarrow 12H^+ + 12e^- + 2CO_2$$

$$\textit{Cathode}: \quad 3O_2 + 12H^+ + 12e^- \rightarrow 6H_2O$$

$$\textit{Overall Reaction}: \quad C_2H_5OH + 3O_2 \rightarrow 2CO_2 + 3H_2O$$

2.2.9 Microbial Fuel Cell :

A microbial fuel cell is a bio electrochemical system that produces electrical energy by using bacteria and their interaction with nature. Microbial electrodes are two types - mediated and unmediated.

In mediated microbial fuel cells where microbials are chemically inactive, electron transfer is facilitated to the electrode from the microbial cell by externally added mediators such as thionine, methyl viologen, methyl blue, humic acid and neutral red (3-Amino-7-dimethylamino-2-methylphenazine hydrochloride). In unmediated microbial fuel cell or mediator free microbial fuel cells electrons are transported directly form the electrochemically active bacterial respiratory enzyme to the electrode. Among the electrochemically active bacteria are *Shewanella putrefaciens*, *Aeromonas hydrophila*, *Gammaproteobacteri*a etc.

In aerobic conditions microorganisms produces carbon dioxide and water by consuming substances such as sugar. But in anerobic condition in the absence of oxygen the produce carbon dioxide, hydrogen ions and electrons. It can be shown as:

$$C_6H_{12}O_6 + 13H_2O \rightarrow 12CO_2 + 48H^+ + 48e^-$$

In mediated microbial fuel cells inorganic mediators begins to liberate electrons from the electron transport chain of the cells after crossing the outer lipid membrane and the bacterial outer membrane. Otherwise those electrons would have been taken up by oxygens. In MFC operation, the anode is the terminal electron acceptor recognized by bacteria in the anodic chamber. Therefore, the microbial activity is strongly dependent on the anode's redox potential. A Michaelis-Menten curve was obtained between the anodic potential and the power output of an acetate-driven MFC. A critical anodic potential seems to provide maximum power output.

2.2.10 Enzymatic Bio Fuel Cell :

An enzymatic biofuel cell specifically uses enzymes as catalysts to oxidize its fuel rather than conventional precious metal electrodes. Though currently confined to research facilities, enzymatic bio fuel cells are most widely prized for the promise they hold in terms of their relatively inexpensive components and fuels, as well as a potential energy source for bionic implants.

General working principle of the enzymatic fuel cell is same as all fuel cells: They use a catalyst to strip electron from the parent fuel molecule and force the electron to go around an electrolyte barrier through a wire to produce electric power. Enzymatic bio fuel

cells uses enzymes derived from living cells but it does not use that enzyme within the cell like in Microbial fuel cell. In order to produce sustainable electrochemical reactions the enzymes must be immobilized near the elctrodes to transfer and accept electrons with anode and cathode respectively. One potential hurdle is large size of enzymes decreases the efficiency of the cell and to combat that problem more three dimensional electrode space was provided for the attachment of large chain enzymes to the electrode for efficient transfer of electrons.

2.2 Types of Fuel for Fuel cell:

Most of the membrane based low temperature fuel cells use hydrogen gas as their fuel source. Alkaline fuel cells and proton exchange membrane fuel cells use commercially available hydrogen.

Phosphoric acid fuel cells and solid acid fuel cells use hydrogen obtained from externally reformed hydrocarbon fuels like diesel or industrial grade propane. They also require external shift conversion of CO to hydrogen to avoid electrolyte contamination and electrode poisoning.

In solid oxide fuel cells and molten carbonate fuel cells the high temperatures help the use light hydrocarbon fuels such as methane, propane and butane by internal reformation. Heavier hydrocarbons like gasoline, diesel, jet fuel (JP-8) or biofuels can be used after reforming them externally.

In direct alcohol fuel cells are characterized by the name of the fuels they use. Direct ethanol fuel cells use ethanol as the source of fuel. Direct methanol fuel cells use methanol as fuel. In both cases the alcohol fuel is used without any internal or external reformation to convert it to hydrogen.

In microbial fuel cell and the enzymatic bio fuel cell uses glucose or alcohols derived from fermentation of glucose products.

In direct carbon fuel cells -a design conceived through the working principle of the solid oxide fuel cells, solid carbon (presumably a fuel derived from coal, pet-coke or biomass) is used directly in the anode, without an intermediate gasification step.

2.3 Electrocatalytic Material For Anode and Cathode:

Electrocatalytic surfaces of the anode and the cathode electrode are the heart of the fuel cell where the main sustainable electrochemical reactions occur to provides a stable flow of electron flux through the external circuit to provide electrical power. Electrocatalytic materials can be categorized into two main parts : Noble or precious metal base electrodes and non-noble metal base electrodes.

2.3.1 Precious base metal for fuel cell:

Any state of the art proton exchange membrane fuel cell now a days uses precious metal like platinum and platinum based alloy electrodes. Tian et al (2017) has discussed new techniques of developments in unsupported platinum (Pt)-based nanocatalysts, with an emphasis on the multidimensional Pt architectures as an alternative to carbon-supported Pt electrocatalysts. The properties of the catalyst material largely depend on their crystalline and electronic structure. Platinum Group Metals are excellent candidates due to their outstanding performance in chemical reactions. Those include oxidative amination, chemoselective reduction, electrophilic cyclization, asymmetric hydrogenation, C-H activation and A^3 coupling. Facets, structure and compositional control of the designed PGMs affects the Oxygen Reduction Reaction (ORR) in terms of catalytic performance. Platinum bimetallic catalysts, core shell nanostructured catalysts, Platinum nano structured materials synthesized by dealloy process and supportless catalysts of Platinum nanostructures like Pt/Pd and Pt/Cu/Co/Ni nanotubes made by templating method based on porous anodic aluminium oxide or galvanic replacement have been explored by Wu et al (2013). Bajpai et al. (2011) [3] investigated the electrochemical and electrical properties of Graphene Supported Platinum Nanoparticle Counter-Electrode for Enhanced Performance of Dye-Sensitized Solar Cells where nanoparticles were deposited directly on to graphene using pulsed laser ablation method (PLD). Guo et al. (2010) [4] proposed a Platinum Nanoparticle Ensemble-on-Graphene Hybrid Nanosheet (PNEGHNs) as new electrode material. Wang et al (2011) [17] investigated the preparation of high-quality reduced

graphene oxide-nanocrystalline platinum hybrid materials by simultaneous co-reduction of graphene oxide and chloroplatinic acid. Bing et al. (2010) [28] investigated nanostructured Pt-alloy electrocatalysts for PEM fuel cell oxygen reduction reaction. The nanostructured Pt-alloy catalysts can be grouped into different clusters: (i) Pt-alloy nanoparticles, (ii) Pt-alloy nanotextures such as Pt-skins/monolayers on top of base metals, and (iii) branched or anisotropic elongated Pt or Pt-alloy nanostructures. Luo et al. (2006) [30] investigated the catalytic activity and the bimetallic composition of carbon-supported gold–platinum (AuPt/C) nanoparticles (2–4 nm diameters) for the electrocatalytic oxygen reduction reaction. Hu et al. (2011) [34] investigated bimetallic Pt–Au nanocatalysts electrochemically deposited on graphene and their electrocatalytic characteristics towards oxygen reduction and methanol oxidation.

2.3.2 Metallic base Fuel cell Electrode:

The free energy diagrams of ORR reaction of tri-metallic sandwich like structures of Pd-Fe-W and Au-Ru-W designed by Ortigoza were plotted based on Density Function Theory. All reactions steps on the afore mentioned two electrodes have shown to be exothermic compared to the last two steps for platinum which are endothermic.with significant thermodynamic barriers (0.15 eV to 0.2eV), henceforth indicating that the proposed materials to be more active towards ORR than platinum. Lefèvre et al investigated the microporous carbon-supported iron based catalyst compared to Pt based catalysts for PEMEFCs and observed sufficiently good ORR of the developed electrode. The predicted the activity is due to iron cation coordination by pyridinic Nitrogen functionalities in the interstices of graphitic sheets within the micropores. Paul and Ghosh (2015) [1] investigated the electrochemical characteristics of electrodeposited MnO_2 at different current densities as electrocatalytic energy material for fuel cell electrode to produce clean alternative green energy from synthesized bio alcohol. Electrochemical characterization of Ni-Co and Ni-Co-Fe electrodeposited on Al foil substrate at optimum condition from an electrolyte of Ni, Co, Fe salts for oxidation of methyl alcohol fuel with high energetic catalytic surface was investigated by Paul et al. (2014) [2]. The use of Co_3O_4 nanomaterial as anode in Li-ion batteries and gas sensors was investigated by Li et al. (2005) [5]. Co_3O_4 nanotubes exhibit excellent sensitivity towards hydrogen and alcohol, owing to their hollow

nanostructured character. Zhu et al. (2000) [12] investigated the sonochemical synthesis of SnO_2 nanoparticles and their preliminary study as Li insertion electrodes. Murray et al. (1999) [19] investigated a direct-methane fuel cell with a ceria-based anode. Fuel cells constitute an attractive power-generation technology that converts chemical energy directly and with high efficiency into electricity while causing little pollution. Park et al. (2000) [20] investigated direct oxidation of hydrocarbons (methane, ethane, 1-butene, n-butane and toluene) at 973 K and 1,073 K with a composite anode of copper and ceria (or samarium-doped ceria).in a solid-oxide fuel cell. Pakapongpan et al. (2017) [24] investigated Magnetic Nanoparticles (Fe_3O_4 NPs)-Reduced Graphene Oxide Nanocomposite as a novel bioelectrode for mediatorless-membraneless glucose Enzymatic biofuel cells. Luo et al. (2008) [27] investigated the Core/shell nanoparticles (Au@Pt, Pt@Au, Fe_3O_4@Au@Pt) as electrocatalysts for fuel cell reactions. Wanjala et al. (2010) investigated nanoscale Alloying, Phase-Segregation, and Core− Shell Evolution of Gold− Platinum Nanoparticles and Their Electrocatalytic Effect on Oxygen Reduction Reaction. Zhang et al. (2011) [32] investigated the Pd–Ni electrocatalysts for efficient ethanol oxidation reaction in alkaline electrolyte. Das et al. (2008) [33] investigated mechanism of potentiostatic deposition of MnO_2 layer on platinum and carbon and electrochemical characteristics of the deposit in relation to carbohydrate oxidation. Kumar et al. (2008) [35] investigated the synthesis and characterization of electrodeposited Ni–Pd alloy electrodes for methanol oxidation. Ni–Pd catalysts synthesized were nanocrystalline, single phase, face centered cubic materials, indicating the formation of complete solid solution in the alloy. Compositional analysis of the alloys indicated that the palladium composition of the alloy increased with decrease in current density. The electrocatalysts prepared are active for methanol oxidation in alkaline medium. Guchhait et al. (2015) [36] investigated the Synthesis and characterization of ZnO-Al_2O_3 oxides as energetic electro-catalytic material for glucose fuel cell.

2.4 SYNTHESIS OF ELECTRODE MATERIALS:

The synthesis techniques of properly designed electrocatalytic material according to required crystalline structure or porosity with certain core material and proper phase is the challenge taken up by modern researchers.

Fundamental advances in energy conversion and storage which are full of vigor in meeting outfaces of some environmental phenomena such as global warming and impact of fossil fuels are held by new materials, particularly nanomaterials, which present unique properties as electrodes and electrolytes in many applications such as lithium batteries, solar cells, fuel cells, and supercapacitors.

There are several techniques that can be used to develop thin films of metals and semiconductors in both micro- and nano-structures. Some of these techniques are: sol-gel process, chemical deposition method, hydrothermal method, pyrolysis method, chemical vapor deposition (CVD), electrodeposition method.

2.4.1 Electrodeposition Method:

Electrochemical deposition is a deposition process in which metal ions in a solution are transported by an electric field to coat the surface of a substrate. The deposition process can be either cathodic or anodic reaction depending on the work piece to be coated (cathode or anode). Electrodeposition of nanostructures, eg. nanocrystallines, nanocomposites, amorphous film or layered materials can be obtained by controlling the electrolysis parameters. The most commonly practiced techniques are (a) pulse current deposition to manipulate the growth of deposits, (b) deployment of additives and surfactants to alter the grain size of deposits and (c) nanoparticles inclusion into deposits to form nanocomposites.

1. Pulse current electrodeposition of nanostructured coating

Direct current is the most commonly deployed technique to deposit a metal coating. Recent years have seen the use of pulsating the current to achieve nanostructure coating. The pulse regime parameters include pulse duty, pulse cycle, frequency and its amplitude, cathodic or anodic current, zero current at open-circuit, etc.

Pulsating the deposition current can affects the diffusion layer next to the electrode surface which is in contact with the liquid solution. This will influence the deposition mechanisms of metal deposits such as altering the nucleation process and the subsequent growth of the deposit. Pulsed current can enable the incorporation of nanoparticles to a high content in the coating as well as producing a wider range of alloys, deposit composition and material properties.

2. Nanoparticles in a metal coating to form nanocomposites

Nanosized particles can be incorporated into metallic coating to form nanocomposite coating. Two common processes involved in the incorporation of particles into metallic coatings are (a) physical dispersion of particles in the electrolyte and (b) electrophoresis migration of particles to the work piece supported by surface charged particles. The metal coating can be plain metal, eg. nickel, copper, tin, gold, or alloys and multilayered coatings.Nanoparticles may include metals, alloys, ceramics, metal oxides, nitrides, carbides, etc. The inclusion of nanoparticles into a metal coating is dependent on many electrolysis parameters such as characteristics of the nanoparticle (particle concentration, surface charge, type, shape, size), electrolyte composition (electrolyte concentration, additives, temperature, pH, surfactant type and concentration), current density (direct current, pulsed current, potentiostatic control) and flow hydrodynamics (laminar, turbulent regimes), electrode geometry and electrodeposition reactor, eg. rotating disk electrode rotating cylinder electrode, parallel plate electrodes, etc.

3. Deployment of electrolyte additives and surfactant technology

Electrolyte additives and surfactant technology are keys to the development of nanostructured materials and coatings. Surfactants can be categorised into groups such as: cationic, anionic, non-ionic or amphoteric. Surfactants can be hydrocarbon or fluorocarbon based. In the surface metal finishing industry, electrolyte additives are commonly grouped by names such as brighteners (provide surface finish as matte, semi-matte or bright appearance), surface wetters (reduce surface tension between, reduce coating porosity or liberation of gas bubbles) and stress relievers (relieve compressive or tensile stress of the coating). Additives and surfactants are deployed to affect the

growth of metal deposits, via adsorption or desorption mechanisms. Many metallic coatings are conventionally designed on the macro-scale. By reducing the macro-scale to the nano-scale could provide enhanced surface properties, leading to a longer lasting, lighter weight and more protective coatings. Electrolyte additives and surfactants are used to affect the grain size of coating. The figure shows a polycrystalline *vs.* nanocrystalline coating. A nanocrystalline coating has nm grain size, with enhanced coating performance against an external load.

2.5 Characterization of electrode material:

2.5.1 Electrochemical Characterization:

2.5.1.1 Cyclic Voltammetry:

Cyclic voltammetry , a subcategory of Voltammetry (an electroanalytical method used in analytical chemistry and various industrial process and research) is a potentiodynamic electrochemical measurement. In voltammetry , information about an analyte is obtained by measuring the current as the potential is varied. Where as in linear sweep voltammetry the experiment concludes when the set potential is reached , in cyclic voltammetry the potential of the working electrode is ramped up to the set potential and then ramped back to the initial potential linearly and is measured against a specific reference potential.

The experiment's scan rate (V/s) is given by the rate of change voltage over time during the voltage sweep between the initial and final set potential. The data plots the current (i) (between working and the counter electrode) versus applied potential (E, which is measured between the working electrode and the reference electrode and often referred to as just 'potential'). In Figure 2, From t_0 to t_1 an linearly increasing reduction potential is applied during the initial forward scan; as a result the cathodic current will, at least initially, increase over this time period assuming that there are reducible analytes in the system. After the reduction potential of the analyte is reached, the cathodic current will decrease as the concentration of reducible analyte is depleted. For a reversible the redox couple during the reverse scan (from t_1 to t_2) the reduced analyte will start to be re-oxidized and it will give rise to a current of reverse polarity (anodic current) to before. The greater reversibility

of the redox couple will lead to the more alike the oxidation peak and the reduction peak. Hence, CV data can provide information about redox potentials and electrochemical reaction rates.

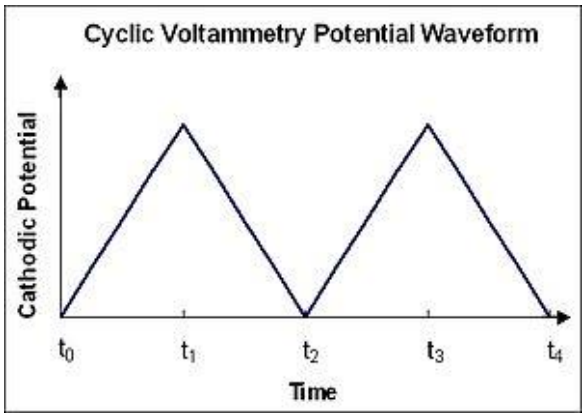

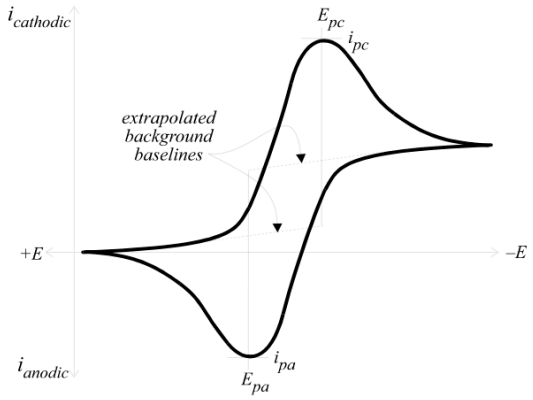

FIGURE 1.1: A CYCLIC VOLTAMMOGRAM

The peak current will be proportional to the square root of the scan rate when the electron transfer at the working electrode surface is fast and the current is limited by the diffusion of analyte species to the electrode surface This relationship is described by the Randles–Sevcik equation. In this situation, the CV experiment only samples a small portion of the solution, i.e., the diffusion layer at the electrode surface.

Often the analyte displays a reversible CV wave (such as that depicted in Figure 1.1), which is observed when all of the initial analyte can be recovered after a forward and reverse scan cycle. Although such reversible couples are simpler to analyze, they contain less information than more complex waveforms.

The waveform of even reversible couples is complex owing to the combined effects of polarization and diffusion. The difference between the two peak potentials (E_p), ΔE_p, is of particular interest.

$$\Delta E_p = E_{pa} - E_{pc} > 0$$

This difference mainly results from the effects of analyte diffusion rates. In the ideal case of a reversible 1e- couple, ΔE_p is 57 mV and the full-width half-max of the forward scan peak is 59 mV. Typical values observed experimentally are greater, often approaching 70 or 80 mV. The waveform is also affected by the rate of electron transfer, usually

discussed as the activation barrier for electron transfer. In an ideal system the relationships reduces to $E_{pa} - E_{pc} = \frac{56.5}{n} mV$ for an *n* electron process.

Focusing on current, reversible couples are characterized by $i_{pa}/i_{pc} = 1$.

When a reversible peak is observed, thermodynamic information in the form of a half cell potential $E^0_{1/2}$ can be determined. When waves are semi-reversible (i_{pa}/i_{pc} is close but not equal to 1), it may be possible to determine even more specific information (see electrochemical reaction mechanism).

Many redox processes observed by CV are quasi-reversible or non-reversible. In such cases the thermodynamic potential $E^0_{1/2}$ is often deduced by simulation. The irreversibility is indicated by $i_{pa}/i_{pc} \neq 1$. Deviations from unity are attributable to a subsequent chemical reaction that is triggered by the electron transfer. Such EC processes can be complex, involving isomerization, dissociation, association, etc.

In cyclic voltammetry, the Randles–Sevcik equation describes the effect of scan rate on the peak current i_p. For simple redox events such as the ferrocene/ferrocenium couple, i_p depends not only on the concentration and diffusional

i_p = current maximum in amps.

$$i_p = 0.4463nFAC\left(\frac{nFvD}{RT}\right)^{\frac{1}{2}}$$

- n = number of electrons transferred in the redox event (usually 1)
- A = electrode area in cm^2
- F = Faraday Constant in C mol^{-1}
- D = diffusion coefficient in cm^2/s
- C = concentration in mol/cm^3
- v = scan rate in V/s
- R = Gas constant in J K^{-1} mol^{-1}

- T = temperature in K

For novices in electrochemistry, the predictions of this equation appear counter-intuitive, i.e. that i_p increases at faster voltage scan rates. It is important to remember that current, i, is charge (or electrons passed) per unit time. In cyclic voltammetry, the current passing through the electrode is limited by the diffusion of species to the electrode surface. This diffusion flux is influenced by the concentration gradient near the electrode. The concentration gradient, in turn, is affected by the concentration of species at the electrode, and how fast the species can diffuse through solution. By changing the cell voltage, the concentration of the species at the electrode surface is also changed, as set by the Nernst equation. Therefore, a faster voltage sweep causes a larger concentration gradient near the electrode, resulting in a higher current.

2.5.1.2 Chronoamperometry:

Chronoamperometry is an electrochemical technique in which the potential of the working electrode is stepped and the resulting current from faradaic processes occurring at the electrode (caused by the potential step) is monitored as a function of time. The functional relationship between current response and time is measured after applying single or double potential step to the working electrode of the electrochemical system. Limited information about the identity of the electrolyzed species can be obtained from the ratio of the peak oxidation current versus the peak reduction current. However, as with all pulsed techniques, chronoamperometry generates high charging currents, which decay exponentially with time as any RC circuit. The Faradaic current - which is due to electron transfer events and is most often the current component of interest - decays as described in the Cottrell equation. In most electrochemical cells this decay is much slower than the charging decay-cells with no supporting electrolyte are notable exceptions.

specifically cortell-equation describes the current response when the potential is a step function. It was derived by Frederick Gardner Cottrell in 1903. For a simple redox event, such as the ferrocene/ferrocenium couple, the current measured depends on the rate at which the analyte diffuses to the electrode. That is, the current is said to be "diffusion

controlled." The Cottrell equation describes the case for an electrode that is planar but can also be derived for spherical, cylindrical, and rectangular geometries by using the corresponding Laplace operator and boundary conditions in conjunction with Fick's second law of diffusion

The Cottrel equation is given by : $i = \frac{nFAc_j^0\sqrt{D_j}}{\sqrt{\pi t}}$

Where, i = current, in unit A

n = number of electrons (to reduce/oxidize one molecule of analyte j, for example)

F = Faraday constant, 96485 C/mol

A = area of the (planar) electrode in cm^2

c_j^0 = initial concentration of the reducible analyte j in mol/cm^3;

D_j = diffusion coefficient for species j in cm^2/s

t = time in s.

Deviations from linearity in the plot of i vs $t^{-1/2}$ sometimes indicate that the redox event is associated with other processes, such as association of a ligand, dissociation of a ligand, or a change in geometry.

In practice, the Cottrell equation simplifies to

$i = kt^{-1/2}$, where k is the collection of constants for a given system (n, F, A, c_j^0, D_j).

Most commonly a three electrode system is used. Since the current is integrated over relatively longer time intervals, chronoamperometry gives a better signal to noise ratio in comparison to other amperometric techniques.

There are two types of chronoamperometry that are commonly used, controlled-potential chronoamperometry and controlled-current chronoamperometry. Before running

controlled-potential chronoamperometry, cyclic voltametries are run to determine the reduction potential of the analytes. Generally, chronoamperometry uses fixed area electrodes, which is suitable for studying electrode processes of coupled chemical reactions, especially the reaction mechanism of organic electrochemistry

2.5.1.3 Potentiodynamic Polarization:

Potentiodynamic is a term describing the measured change in the electrical potential (voltage) of a system. In electrochemistry, this term is used in describing polarization methods in the corrosion industry. Potentiodynamic polarization refers to a polarization technique in which the potential of the electrode is varied over a relatively large potential domain at a selected rate by the application of a current through the electrolyte. Potentiodynamic polarization is often used for laboratory corrosion testing. It can provide significant useful information regarding corrosion mechanisms, corrosion rate and susceptibility of specific materials to corrosion in designated environments.

Tafel extrapolation and polarization resistance are two methods to measure corrosion rates. Polarization methods are faster experimental techniques compared to classical weight loss estimation. Tafel relationship with respect to activation controlled anodic and cathodic processes has been discussed earlier. For an electrochemical reaction under activation control, polarization curves exhibit linear behavior in the E Vs log (i) plots called Tafel behavior. Typical polarization behavior of metals in acid solution in the presence and absence of oxygen are illustrated below.

The net exchange current density considering both anodic and cathodic currents is given by Butler-Volmer equation and is given by as follows:

$$j = j_0 \cdot \left\{ e^{\left[\frac{\alpha_a zF}{RT}(E - E_{eq}) \right]} - e^{\left[-\frac{\alpha_c zF}{RT}(E - E_{eq}) \right]} \right\}$$

in more compact form: $$j = j_0 \cdot \left\{ e^{\left[\frac{\alpha_a zF}{RT}\eta \right]} - e^{\left[-\frac{\alpha_c zF}{RT}\eta \right]} \right\}$$

where,

- j : electrode current density
- j_0: echange current densaity
- E : electrode potential ,V
- E_{eq}: Equilibrium Potential
- T: Absolute temperature, K
- z: number of electrons involved in electrode reacton
- F: Faraday Constant
- R: Universal Gas Constant
- α_c: Cathodic charge transfer coefficient
- α_a: anodic charge transfer coefficient
- η: activation over potential (defined as $\eta = E - E_{eq}$

This form of Butler-Volmer equation is only valid for electrically charge controlled reaction on the electrode surface. When mass transfer between electrode and the bulk of the electrolyte or analyte system is in control of the electrode reaction the electrode current is modified with limiting current density given by : $j_{limiting} = \frac{zFD_{eff}}{\delta} c^*$

where:

- D_{eff} is the effective diffusion coefficient (taking tortuosity into account, if any);
- δ is the diffusion layer thickness;
- c^* is the concentration of the electroactive (limiting) species in the bulk of the electrolyte

The modified most general form of Butler -Volmer accounting for mass transfer controlled reaction is given by:

$$j = j_0 \left\{ \frac{C_o(0,t)}{C_o^*} e^{\left[\frac{\alpha_a zF\eta}{RT}\right]} - \frac{C_r(0,t)}{C_r^*} e^{\left[-\frac{\alpha_c zF\eta}{RT}\right]} \right\}$$

where:

- j is the current density, A/m^2,
- C_o and C_r refer to the concentration of the species to be oxidized and to be reduced, respectively,
- C (0, t) is the time-dependent concentration at the distance zero from the surface.

The above form simplifies to the conventional one (shown at the top of the article) when the concentration of the electroactive species at the surface is equal to that in the bulk.

2.5.1.4 Electrochemical Impedance Spectroscopy:

Any electrochemical system can be analyzed by comparing it with an equivalent electrical circuit consisting of some specific type of equivalent circuit elements. Electrochemical impedance of the electrochemical system under investigation is usually measured by applying an AC potential to an electrochemical cell and then measuring the current through the cell. Assume that we apply a sinusoidal potential excitation. The response to this potential is an AC current signal. This current signal can be analyzed as a sum of sinusoidal functions (a Fourier series).

Electrochemical impedance is normally measured using a small excitation signal such as $E_t = E_0 \sin(\omega t)$ where E_t is the potential at time t, E_0 is the amplitude of the signal, and ω is the radial frequency expressed as: $\omega = 2\pi f$. The relationship between radial frequency ω (expressed in radians/second) and frequency f (expressed in hertz) is:. This is done so that the cell's response is pseudo-linear. In a linear (or pseudo-linear) system, the current response to a sinusoidal potential will be a sinusoid at the same frequency but shifted in phase (see Figure 1) and is given by $I_t = I_0 \sin(\omega t - \varphi)$. In a linear system, the response signal, I_t, is shifted in phase (Φ) and has a different amplitude than I_0. Linearity is described in more detail in the following section. An analogous to ohms law to calculate the impedance of the system is given by:

$$Z_t = \frac{E_t}{I_t} = \frac{E_0 \sin(\omega t)}{I_0 \sin(\omega t + \varphi)} = Z_0 \frac{\sin(\omega t)}{\sin(\omega t + \varphi)}$$

The plot of sinusoidal excitation signal E_t and φ angle phase shifted response signal I_t on x-axis and y-axis respectively produces and oval figure often known as "Lissajous Figure", which was the accepted method of EIS technique on oscilloscope prior to modern EIS instrumentation. Using Euler's relationship of complex number representation; if excitation voltage signal and response current signal is taken as complex signals $E_t = E_0 e^{(i\omega t)}$ and $I_t = I_0 e^{(i(\omega t - \varphi))}$ then the impedance can be represented as a complex number by following:

$$Z_t = \frac{E_t}{I_t} = \frac{E_0 \, e^{(i\omega t)}}{I_0 e^{(i(\omega t - \varphi))}} = Z_0 e^{\varphi} = Z_0(\sin\varphi + \cos\varphi)$$ and if plotted for a simple circuit with a characteristic of single time constant with real part on x-axis and imaginary part on y-axis then we get the following figure:

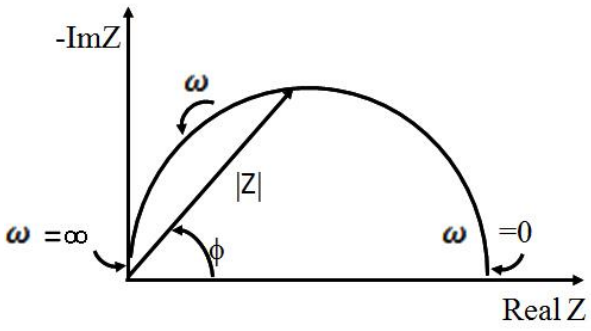

Figure 1: Nyquist Plot of a Simple circuit

Nyquist Plots have one major shortcoming. When you look at any data point on the plot, you cannot tell what frequency was used to record that point.

Another popular presentation method is the Bode Plot, where, impedance is plotted with log frequency on the X-axis and both the absolute values of the impedance ($|Z|=Z_0$) and the phase-shift on the Y-axis., showing frequency information unlike Nyquist plot.

2.5.2.Material Characterization:

2.5.2.1 X-Ray Diffraction:

X-ray powder diffraction (XRD) is a rapid analytical technique primarily used for phase identification of a crystalline material and can provide information on unit cell dimensions. The analyzed material is finely ground, homogenized, and average bulk composition is determined.

Max von Laue, in 1912, discovered that crystalline substances act as three-dimensional diffraction gratings for X-ray wavelengths similar to the spacing of planes in a crystal lattice. X-ray diffraction is now a common technique for the study of crystal structures and atomic spacing.

X-ray diffraction is based on constructive interference of monochromatic X-rays and a crystalline sample. These X-rays are generated by a cathode ray tube, filtered to produce monochromatic radiation, collimated to concentrate, and directed toward the sample. The interaction of the incident rays with the sample produces constructive interference (and a diffracted ray) when conditions satisfy BraggMax von Laue, in 1912, discovered that crystalline substances act as three-dimensional diffraction gratings for X-ray wavelengths similar to the spacing of planes in a crystal lattice. X-ray diffraction is now a common technique for the study of crystal structures and atomic spacing.

X-ray diffraction is based on constructive interference of monochromatic X-rays and a crystalline sample. These X-rays are generated by a cathode ray tube, filtered to produce monochromatic radiation, collimated to concentrate, and directed toward the sample. The interaction of the incident rays with the sample produces constructive interference (and a diffracted ray) when conditions satisfy Bragg's Law ($n\lambda=2d\sin\theta$). This law relates the wavelength of electromagnetic radiation to the diffraction angle and the lattice spacing in a crystalline sample. These diffracted X-rays are then detected, processed and counted. By scanning the sample through a range of 2θangles, all possible diffraction directions of the lattice should be attained due to the random orientation of the powdered material. Conversion of the diffraction peaks to d-spacings allows identification of the mineral because each mineral has a set of unique d-spacings. Typically, this is achieved by comparison of d-spacings with standard reference patterns.

All diffraction methods are based on generation of X-rays in an X-ray tube. These X-rays are directed at the sample, and the diffracted rays are collected. A key component of all diffraction is the angle between the incident and diffracted rays. Powder and single crystal diffraction vary in instrumentation beyond this.

Bragg's Law ($n\lambda=2d \sin\theta$). This law relates the wavelength of electromagnetic radiation to the diffraction angle and the lattice spacing in a crystalline sample. These diffracted X-rays are then detected, processed and counted. By scanning the sample through a range of 2θangles, all possible diffraction directions of the lattice should be attained due to the random orientation of the powdered material. Conversion of the diffraction peaks to d-spacings allows identification of the mineral because each mineral has a set of unique d-spacings. Typically, this is achieved by comparison of d-spacings with standard reference patterns.

All diffraction methods are based on generation of X-rays in an X-ray tube. These X-rays are directed at the sample, and the diffracted rays are collected. A key component of all diffraction is the angle between the incident and diffracted rays. Powder and single crystal diffraction vary in instrumentation beyond this.

X-ray diffractometers consist of three basic elements: an X-ray tube, a sample holder, and an X-ray detector.

X-rays are generated in a cathode ray tube by heating a filament to produce electrons, accelerating the electrons toward a target by applying a voltage, and bombarding the target material with electrons. When electrons have sufficient energy to dislodge inner shell electrons of the target material, characteristic X-ray spectra are produced. These spectra consist of several components, the most common being K_α and K_β. K_α consists, in part, of $K_{\alpha1}$ and $K_{\alpha2}$. $K_{\alpha1}$ has a slightly shorter wavelength and twice the intensity as $K_{\alpha2}$. The specific wavelengths are characteristic of the target material (Cu, Fe, Mo, Cr). Filtering, by foils or crystal monochrometers, is required to produce monochromatic X-rays needed for diffraction. $K_{\alpha1}$and $K_{\alpha2}$ are sufficiently close in wavelength such that a weighted average of the two is used. Copper is the most common target material for single-crystal diffraction, with CuK_α radiation = 1.5418Å. These X-rays are collimated and directed onto the sample. As the sample and detector are rotated, the intensity of the

reflected X-rays is recorded. When the geometry of the incident X-rays impinging the sample satisfies the Bragg Equation, constructive interference occurs and a peak in intensity occurs. A detector records and processes this X-ray signal and converts the signal to a count rate which is then output to a device such as a printer or computer monitor.

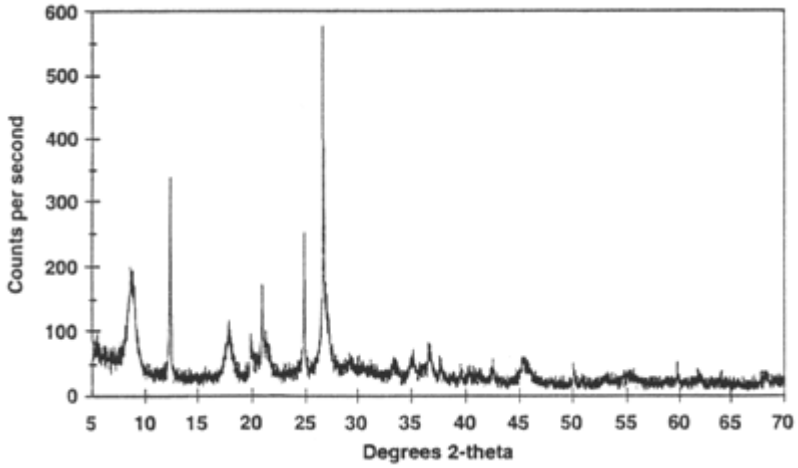

The geometry of an X-ray diffractometer is such that the sample rotates in the path of the collimated X-ray beam at an angle θ while the X-ray detector is mounted on an arm to collect the diffracted X-rays and rotates at an angle of 2θ. The instrument used to maintain the angle and rotate the sample is termed a *goniometer*. For typical powder patterns, data is collected at 2θ from ~5° to 70°, angles that are preset in the X-ray scan.

X-ray powder diffraction is most widely used for the identification of unknown crystalline materials (e.g. minerals, inorganic compounds). Determination of unknown solids is critical to studies in geology, environmental science, material science, engineering and biology.

2.5.2.2 Scanning Electron Microscopy:

The scanning electron microscope (SEM) uses a focused beam of high-energy electrons to generate a variety of signals at the surface of solid specimens. The signals that derive from electron-sample interactions reveal information about the sample including external morphology (texture), chemical composition, and crystalline structure and orientation of materials making up the sample. In most applications, data are collected over a selected area of the surface of the sample, and a 2-dimensional image is generated that displays spatial variations in these properties. Areas ranging from approximately 1 cm to 5

microns in width can be imaged in a scanning mode using conventional SEM techniques (magnification ranging from 20X to approximately 30,000X, spatial resolution of 50 to 100 nm). The SEM is also capable of performing analyses of selected point locations on the sample; this approach is especially useful in qualitatively or semi-quantitatively determining chemical compositions (using EDS), crystalline structure, and crystal orientations (using EBSD). The design and function of the SEM is very similar to the EPMA and considerable overlap in capabilities exists between the two instruments.

Samples must be solid and they must fit into the microscope chamber. Maximum size in horizontal dimensions is usually on the order of 10 cm, vertical dimensions are generally much more limited and rarely exceed 40 mm. For most instruments samples must be stable in a vacuum on the order of 10^{-5} - 10^{-6} torr. Samples likely to outgas at low pressures (rocks saturated with hydrocarbons, "wet" samples such as coal, organic materials or swelling clays, and samples likely to decrepitate at low pressure) are unsuitable for examination in conventional SEM's. However, "low vacuum" and "environmental" SEMs also exist, and many of these types of samples can be successfully examined in these specialized instruments. EDS detectors on SEM's cannot detect very light elements (H, He, and Li), and many instruments cannot detect elements with atomic numbers less than 11 (Na). Most SEMs use a solid state x-ray detector (EDS), and while these detectors are very fast and easy to utilize, they have relatively poor energy resolution and sensitivity to elements present in low abundances when compared to wavelength dispersive x-ray detectors (WDS) on most electron probe microanalyzers (EPMA). An electrically conductive coating must be applied to electrically insulating samples for study in conventional SEM's, unless the instrument is capable of operation in a low vacuum mode.

2.5.3 Fourier Transform Infrared Spectroscopy

FTIR is a vibrational spectroscopy technique and is described as an absorption technique which emits infrared (IR) frequencies from the near-IR region 14,000–4000cm−1 , the mid-IR region 4000–400cm−1 and the far-IR region 400–10cm−1 . Both macro- and micro-FTIR are used extensively in conservation science—macro is used for bulk analysis and micro, by virtue of the attachment of a microscope, allows spectra to be collected from specific areas of a sample. Micro-FTIR can use transmitted, reflected and attenuated light

to analyze a sample. Transmitted light is applied to very thin samples, reflected light is used when the sample is not suitable for transmission (when it is opaque), and when neither of these modes work, an attenuated total reflection (ATR) mode is used for both micro- and macro-analyses. Larkin describes the principles of FTIR in more detail and additionally compares and contrasts FTIR and Raman in a manner that is informative to scientists and non-scientists alike.

Chapter 3: Experimental Method

Chapter 3:Experimental Method

In this chapter the experimental methods used in this project has been presented in details. The proposed Ni-NiO based electrocatalytic surface was prepared by a two-step method on aluminium substrate.

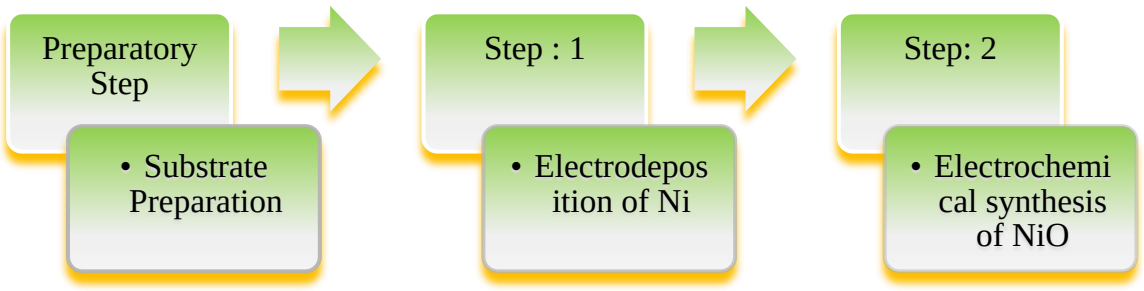

3.1 Raw Materials:

The substrate used in the development of the electrode catalyst is 99.9% industrial grade aluminium foil 2mm thick was cut in the size of 3cmx1cm plate size.

Aluminium was selected as the substrate material because aluminium has better electrical conductivity among easily available metals and comparatively cheaper than next best candidate copper.

3.2 Electrodeposition Method:

Electrodeposition was selected as the synthesis technique for Ni-NiO because it provides the desired outputs in less complicated infrastructure and low cost.

3.2.1 Surface Preparation:

Then the cut substrate, an area of dimension 1cm x 1cm on both sides were polished in 2/0, 3/0 grade silica paper. Then it was boiled in aqueous KOH solution to remove any Al_2O_3 layer on the surface and subsequently rinsed in ethanol and acetone and dried before proceeding for electrodeposition.

3.2.2 Solution Chemistry:

In our present work two electrocatalytic surface was investigated. Our primary target was produce Ni-NiO on aluminium to observe its electrocatalytic effect towards oxidation of glucose based solution. Further addition of electrochemically exfoliated nano graphite sheets were incorcorated with it to investigate the effect of its addition with Ni-NiO. The synthesis method of electrochemically exfoliated graphite has been discussed later.

For step 1 i.e. the electrochemical deposition of Ni, a Ni^{2+} solution bath was prepared. The basic composition of the solution consisted of nickel chloride hexahydrate ($NiCl_2$,$6H_2O$), nickel sulfate hexahydrate ($NiSO_4$,$6H_2O$), boric acid (H_3BO_3) and sodium dodecyl sulfate($C_{12}H_{25}OSO_2ONa$) in distilled water. The conductivity as well as pH of the solution was maintained by addition of measured amount of concentrated Sulfuric acid(H_2SO_4).

For this current investigation Ni deposition of three different of Solution chemistry for Ni bath was prepared as given by the following table.

Chemical	Solution 1	Solution 2	Solution3
$NiCl_2$,$6H_2O$	0.65 M	0.6M	0.70 M
$NiSO_4$,$6H_2O$	0.30 M	0.30M	0.30 M
H_3BO_3	0.90 M	0.90 M	0.90 M
$C_{12}H_{25}OSO_2ONa$	0.001 M	0.001 M	0.001 M

In step 2 the Ni plated aluminium electrodes was electrochemically treated in a solution of Oxalic acid to produce Ni-NiO catalytic surface.

For second investigation to see the effect of electrochemically exfoliated graphite particles deposited on Ni-NiO surface, the graphite powder were synthesized by

electrochemical exfoliation of graphite rods in a solution of 0.1M H_2SO_4 at 10V d.c. voltage applied through a d.c. voltage regulator. For this exfoliation two graphite electrodes were used, one as anode another as cathode. The anode electrode was seen to be exfoliated an produce fine graphite particles which made a black colloid solution with the electrolyte over a certain time of exposure. Then the electrodes were removed from the colloidal electrolyte solution of the graphite and the whole solution was ultra-sonicated in an ultrasonic bath for 1 hour to disperse the particles into more finer form. Then the colloidal solution was filtered and the filtrate was vigorously cleaned with distilled water and dried. Thus obtained electrochemically exfoliated finer graphite powders were expected to have multilayer graphene flakes in them, which was this projects another interest to investigate.as electrocatalytic material.

3.2.3 Experimental Setup

All the experiments were performed in an regulated and temperature controlled set up as possible.

3.2.3.1 Electrodeposition:

The electrodeposition of the Ni was performed by a DC voltage generator which has two terminals -one positive and other negative terminal. For deposition form a specific solution first the solution was taken in a beaker and was heated to a specified temperature before a new depostion.. Then the beaker was mounted on a REMI 500 magnetic stirring assisted heat plate with a steady heating rate to maintain that temperature and a thermometer was inserted to collect continuous temperature reading. The graphite electrode was used as counter electrode which is anode in case of Ni deposition and was connected to the positive terminal of the voltage generator. The pretreated and cleaned substrate was dipped in the solution bath and was connected to the negative terminal of the dc voltage regulator through a multimeter in series by using an alligator clip connector to measure the line current. A lugging capillary salt bridge made of saturated KCl and agar-agar gel containing the reference saturated calomel electrode (SCE) was dipped into the solution bath. The connecting end of the SCE was connected to the ground terminal of an multimeter and the other end of that voltage measuring multimeter was connected in parallel with the substrate end which happens to be the cathode in the solution bath. During the

electrodeposition the constant current density on the working electrode surface (here cathode) was maintained by regulating the voltage.

The deposition reaction can be given as follows:

$$In\,Cathode: Ni^{2+} + 2e^{-} \rightarrow Ni$$

Variation of parameters

Current density , temperature and pH were varied as follows:

Solution Type	Current density (mA/cm^2)	Temperature (ºC)	pH
Solution 1	250	60	2.5-3.5
	300	60	2.5-3.5
	350	60	2.5-3.5
Solution 2	250	60	2.5-3.5
	300	60	2.5-3.5
	350	60	2.5-3.5
Solution 3	250	60	2.5-3.5
	300	60	2.5-3.5
	350	60	2.5-3.5

NiO Coating:

For NiO deposition the the Ni coated electrodes were dried in air and then cleaned thoroughly with ethanol, acetone and distilled water respectively and then dried again after soaking the water with tissue paper. Then the electrodes the interested area of Ni coat was dipped into the 1M Oxalic acid solution connected with an DC Supply. The Ni electrode was made an Anode and a graphite electrode was used as counter cathode and In that oxalic acid solution NiO was deposited at anode with current density of $100mAcm^{-2}$ and Then the electrode was removed and cleaned with distilled water and dried before proceeding to characterization.

3.2.3.2 Addition of electrochemically exfoliated Graphite Particles:

Electrochemically exfoliated graphite particles or multilayer graphene particles were added in the nickel bath at 2gms/50ml of solution and was electrochemically codeposited with Ni. This deposition was facilitated by magnetic stirring.

3.3. Characterization

3.3.1 Electrochemical Characterization:

Electrochemical characterization of the synthesized electrocatalytic surfaces was performed by a 'Versastat 3' potentiostat. It has four terminals each for working electrode, working sense, counter electrode and reference electrode.

Cyclic voltammetry was performed to find out the electrochemical activity of the analyte on the electrode surface. In this case a fuel solution of 0.5M dm^{-3} glucose and 1M dm^{-3} sulfuric acid was taken. The cyclic voltammetric scan was performed form -1V to 1V at a scan rate of 50mV/s.

The chronoamperometry of the electrode was performed at 1V voltage for 1000 secs with a scan rate of 1point per decade in a fuel solution of 0.5M dm^{-3} glucose and 1M dm^{-3} sulfuric acid.

The potentiodynamic polarization of the electrodes was performed in the fuel solution of 0.5M dm^{-3} glucose and 1M dm^{-3} sulfuric acid. The potential was swept from cathodic to anodic polarization with an ASTM standard scan rate of 1mV/sec.

3.3.2. Electrochemical Impedance Spectroscopy:

The electrochemical property in terms of polarization resistance was investigated by performing electrochemical impedance spectroscopy on a Gamry Potentiostat. The electrochemical cell with three electrode system : a working electrode (electrode surface under investigation), a counter electrode (graphite) and a saturated calomel electrode (SCE) all immersed in a fuel solution of 0.5M dm^{-3} glucose and 1M dm^{-3} sulfuric acid was

connected with the corresponding apparatus electrode terminals and experiment was performed.

The data recorded by the potentiostat was stored in a computer and was analyzed by Gamry Echem Analyst software.

3.3.3 Physical Characterization:

3.2.1 XRD:

X-ray diffractometry with Cu (Kα), radiation was used to understand the phases present in the electrode in a "Rigaku Ultima III" X-ray Diffractometer.

3.2.2 Scanning Electron Microscopy:

The developed electrocatalytic material was examined under higher magnification to assess the deposit structure and morphology, deposit nature, heterogeneities , pores present in the deposits using a scanning Electron Microscope of "Hitachi S-4800".

Chapter 4:
Results and Discussions

Chapter 4: Results and Discussions

Present investigation has been carried out by performing electrochemical tests such as Cyclic Voltammetry (CV), Chronoamperometry (CA), Potentiodynamic Polarization (PD) as described in chapter 3 under experimental methods. The Electrochemical Impedance Spectroscopy (EIS) of energetic electrode material so developed was also performed to compute polarization resistance, double layer capacitance, solution resistance. Material characterization of electrode was also performed by XRD and Scanning Electron Microscopy (SEM) to find out the constituents of Ni-NiO-Graphene complex as well as the morphology of substrate structure.

The following paragraph discussed the experimental result, computed data from the experiments and the electrochemical & material science theory to understand the performance of the best performing electrode.

4.1 Cyclic Voltammetry:

The maximum current that can be obtained on oxidation of Glucose fuel over the electrode surface can be understood from the CV curves. Fig 4.1a, 4.1b, 4.1c shows the CV of Ni-NiO electrode produced by varying the current density while keeping the solution bath chemistry fixed.

The glucose is expected to be oxidized to gluconolactone on the electrocatalytic surface giving of hydrogen ion and electron given by the following anode reaction:

$$C_6H_{12}O_6 + H_2O \rightarrow C_6H_{12}O_7 + 2H^+ + 2e^-$$

The complementary cathode reaction is given by:

$$\frac{1}{2}O_2 + 2H^+ + +2e^- \rightarrow H_2O$$

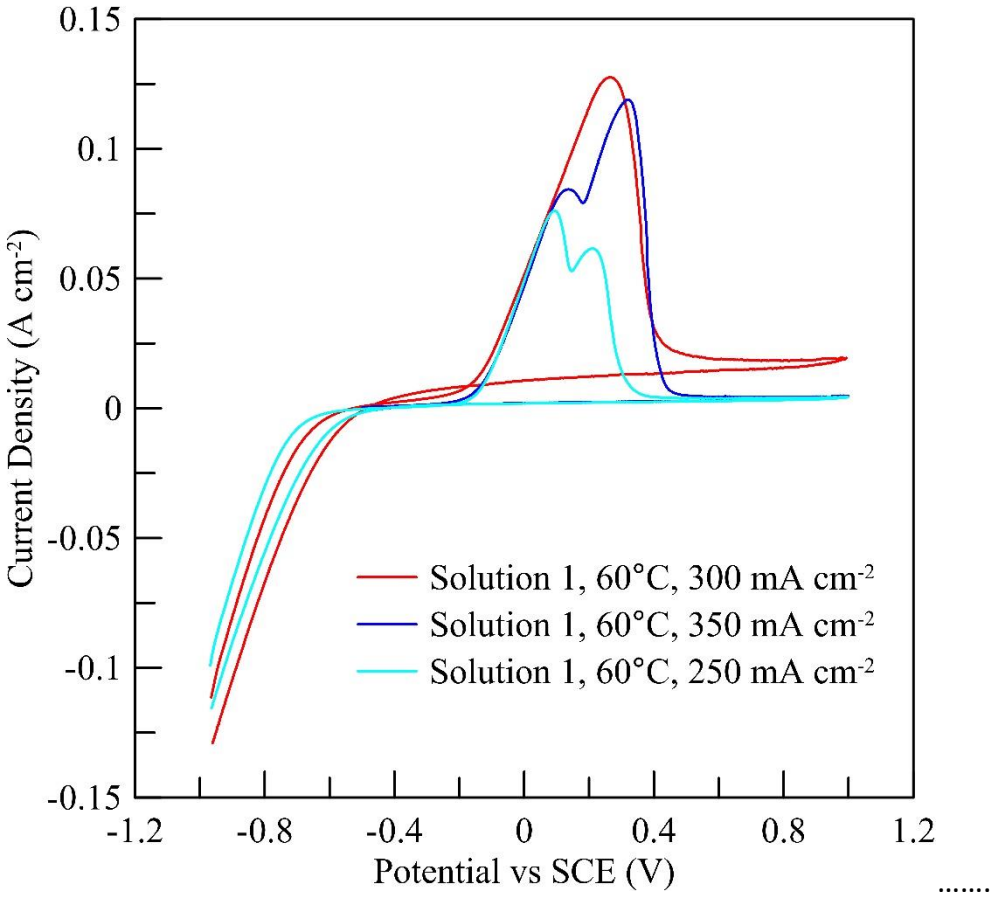

.....

Fig.4.1a: CV of Ni-NiO deposited at Fixed Solution Chemistry 1 bath at varying current densities and at constant temperature of 60ºC

Keeping the current density on the electrodeposition surface of substrate & the temperature of the solution bath fixed, it is seen that all the curves gives a maxima (i_{max}) around a particular potential and this i_{max} increase with deposition current reaching a maximum at an optimum value of current density and there after decreases.

The electrochemical energy content is given by the area under the curve. An increase in current density of electrodeposition supplies more electron charge density on the cathode surface. Now the cation Ni^{2+} accumulated near the electrode surface will be immediately discharged and deposited on the electrode surface by accepting electrons from it. The deposited material that is Ni would be formed by Nucleation and Growth.

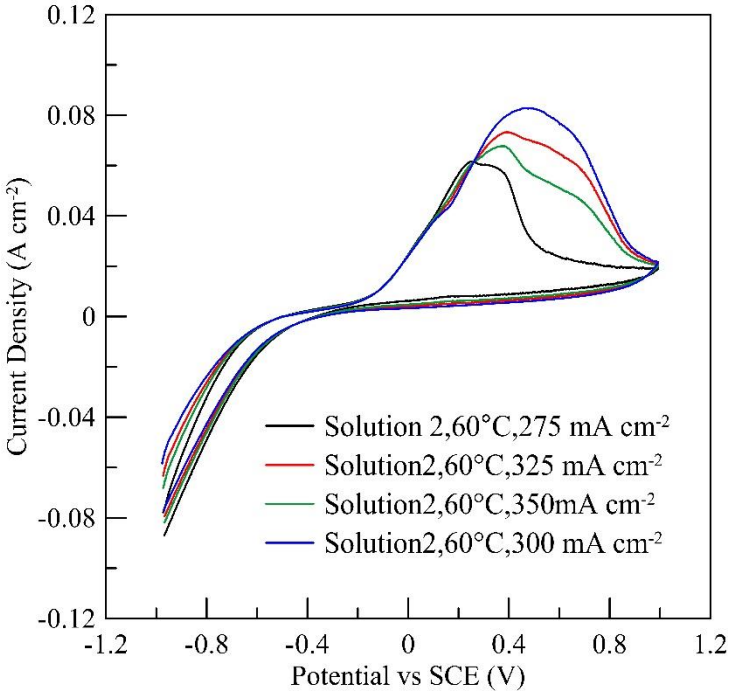

Fig.4.1b: CV of Ni-NiO deposited at Fixed Solution Chemistry 2 bath at varying current density at constant temperature of 60ºC

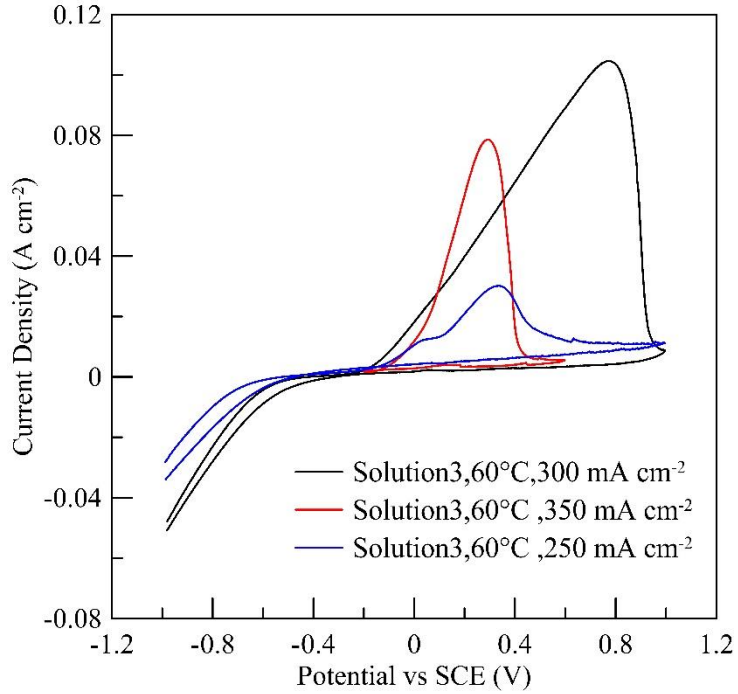

Fig.4.1c: CV of Ni-NiO deposited at Fixed Solution Chemistry 3 bath at varying current density at constant temperature of 60ºC

Deposition potential for the Metallic reduction: $M^{n+} + ne^{-} = M$ is given by the following relation:

$$E_{deposition} = E^0 + \frac{RT}{nF}\log[M^{n+}] + \eta_{Act} + \eta_{Conc} + IR$$

Where,

E^0=Standard Deposition potential	n= Number of electrons involved
R= Universal gas constant	η_{Act}=Activation Overvoltage
T= Absolute temperature	η_{Conc} = Concentration Overvoltage
F= Faraday Constant	IR= Ohmic Resistance Loss

So, the minimum potential to deposit a metal atom is dependent on overvoltage & solution resistance besides the electron potential. If the temp is more, then the concentration overvoltage will decrease as the diffusion boundary layer thickness and mobility of the ion increases due to convection. After all the metal ions at the electrode boundary have been deposited the electrons on the electrode surface need to wait for new ions to diffuse from the bulk of the solution towards the electrode surface need to wait for new ions to diffuse from the bulk of the solution towards the electrode surface. With higher current deposition rates, a greater amount of electrons are accumulated in the electrodes making it highly negatively charged. It will capture charge impurities from the solution or impure gases from the environment such as NH_3, SO_2, CO_2 etc. to reduce its charge and thereby the electrodes are contaminated by small amount of nonconductive impurities entrapped. This decreases the i_{max} a little bit. So that's why it is needed to find out the optimum current density to produce best performed electrodes. Fig 4.1a, 4.1b,4.1c and 4.1d supports that fact.

Electrooxidation of a fuel or analyte in electrochemistry is surface charge transport phenomenon and the catalytic materials affinity towards the material. The greater the electrode surface area provided for oxidation the better will be the catalytic performance. Though electrodeposition allows to synthesize highly oriented 3D surface at nanoscale with a very high surface to volume ratio, it is a sophisticated process. Though the temperature of the deposition bath helps to increase conductivity of the solution by convection, after a certain limit the effect of temperature become detrimental to the growth and structure of the electrodeposited Ni towards the goal of nano-scale deposition. This effect can be observed in the Fig.4.1d and Fig. 4.1e.

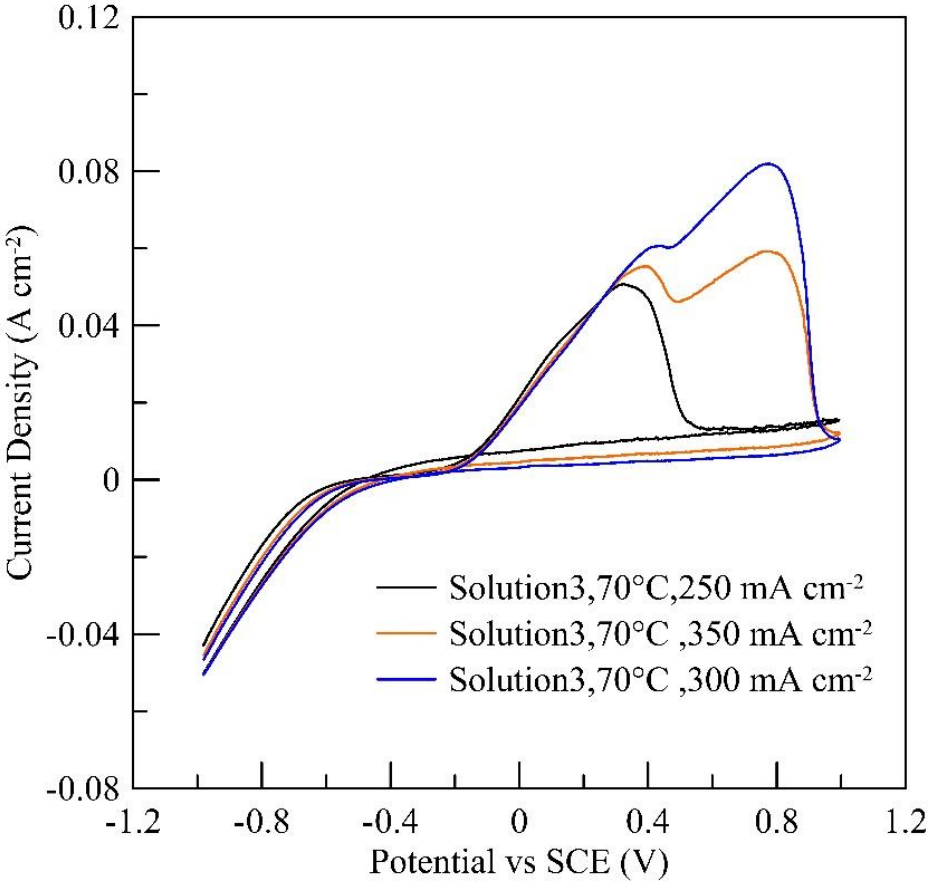

Fig.4.1d : CV of Ni-NiO deposited at Fixed Solution Chemistry 3 bath at varying current density at constant temperature of 70ºC

The effect of temperature of electrodeposition can be observed on the CV graphs of Ni-NiO deposited electrodes in 0.5M glucose and 1M sulfuric acid given by Fig.4.1c and Fig.4.1d. For same solution bath of deposition, and preconditions it is observed that at higher temperature near the same oxidation potential less current is produced.

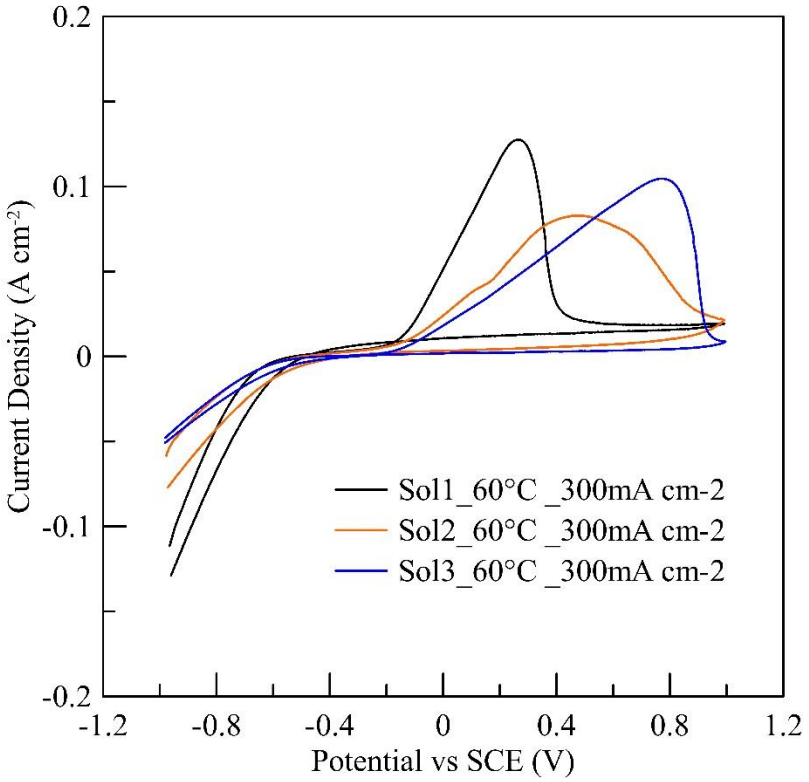

Fig.4.1e : CV of Ni-NiO deposited at varying Solution Chemistry bath at constant current density at constant temperature of 60ºC

Among the three solution baths, Solution 1 seemed to be the best candidate to go for Ni coating for high energetic electrode synthesis according to the Fig.4.1e.The optimum current density is determined by further characterizing the surfaces by other techniques.

4.1.1 Addition of Electrochemically exfoliated graphite on Ni-NiO:

Graphene, a recently developed 2-D allotrope of carbon has been reported to behave as high energetic electrode material. It is thought it will be interesting to see if the graphene is co-deposited along with Ni & NiO. Fig 4.1f gives a comparative CV display of the Ni-NiO electrode material with & without graphene. It is seen that both the maximum current & the energy delivered has the increased by nearly 50%. So, the oxidation of the glucose on the electrode surface with graphene

has produced high current compared to its oxidation on the simple Ni-NiO electrode surface supports the fact that it is a high energetic material.

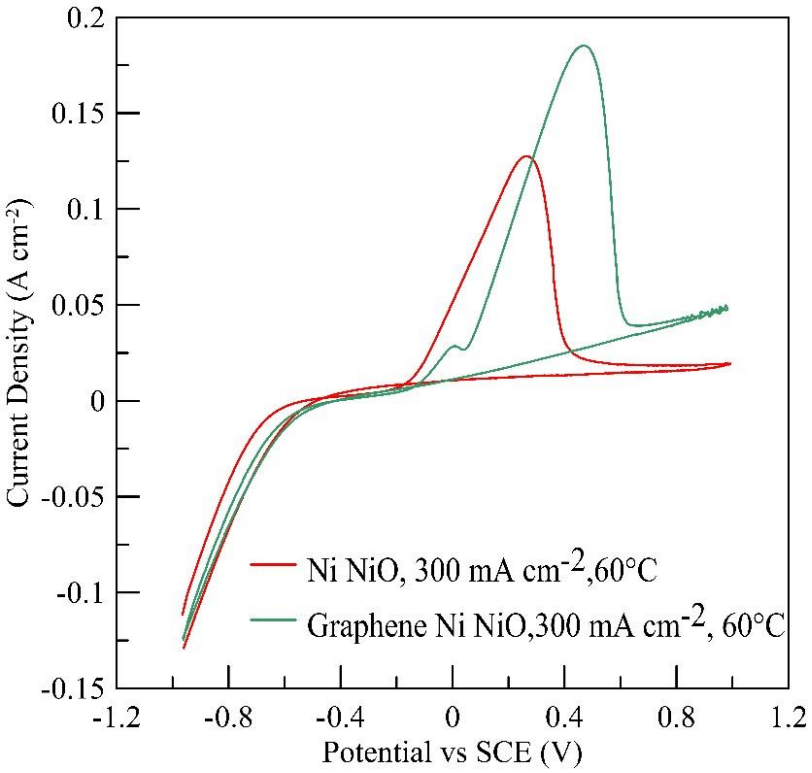

Fig.4.1f: CV of Ni-NiO and Graphene-Ni-NiO deposited at constant current density 300mA cm^{-2} at constant temperature of 60ºC

4.2 Chronoamperometry (CA):

Having obtained high energetic electrode with very good maximum current density and energy content it is interesting to find out how the current decays with time by performing Chronoamperometry test. Any stable electrocatalytic surface produces a steady current for a certain period of time before its surface is contaminated and becomes electrochemically less active. In this work the electrodes synthesized by numerous variations of deposition parameters are tested in 25°C and 45°C fuel solutions of 0.5M glucose and 1M sulfuric acid at constant excitation voltage of 1V and at a scan rate of 1decade/sec. The results are presented as per standard time vs current density in Fig.4.2a, Fig.4.2b and Fig.4.2c.

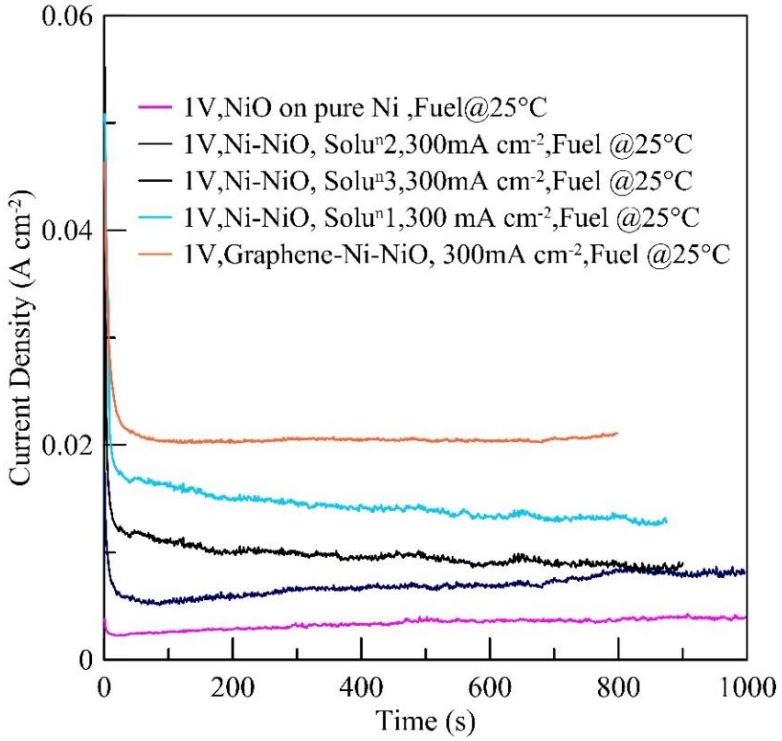

Fig.4.2a: CA of Ni-NiO and Graphene-Ni-NiO deposited at constant current density 300mA cm^{-2} at constant temperature of 60ºC at, tested in 25°C Fuel solution

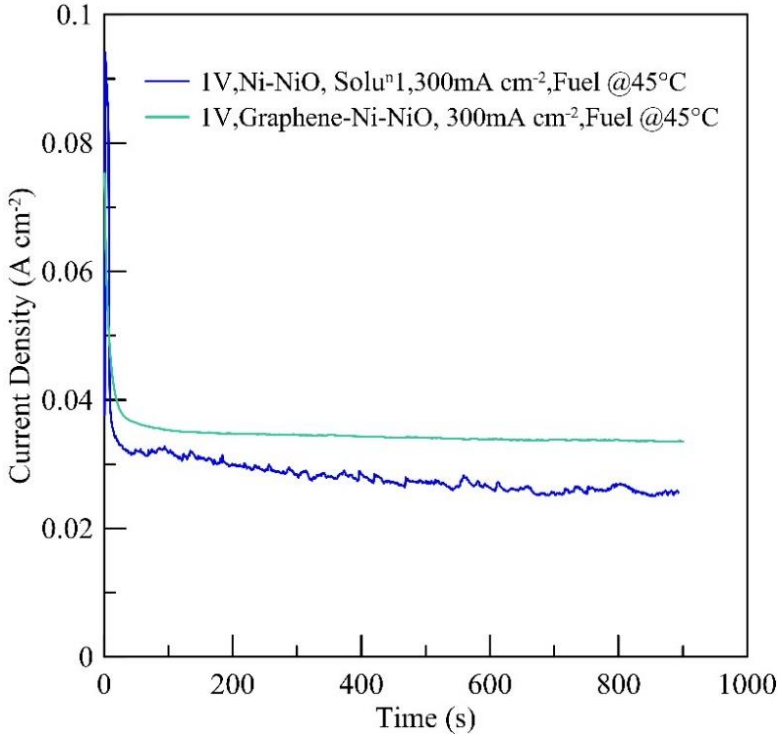

Fig.4.2b: CA of Ni-NiO and Graphene-Ni-NiO deposited at constant current density 300mA cm^{-2} at constant temperature of 60ºC, tested in 45°C Fuel solution

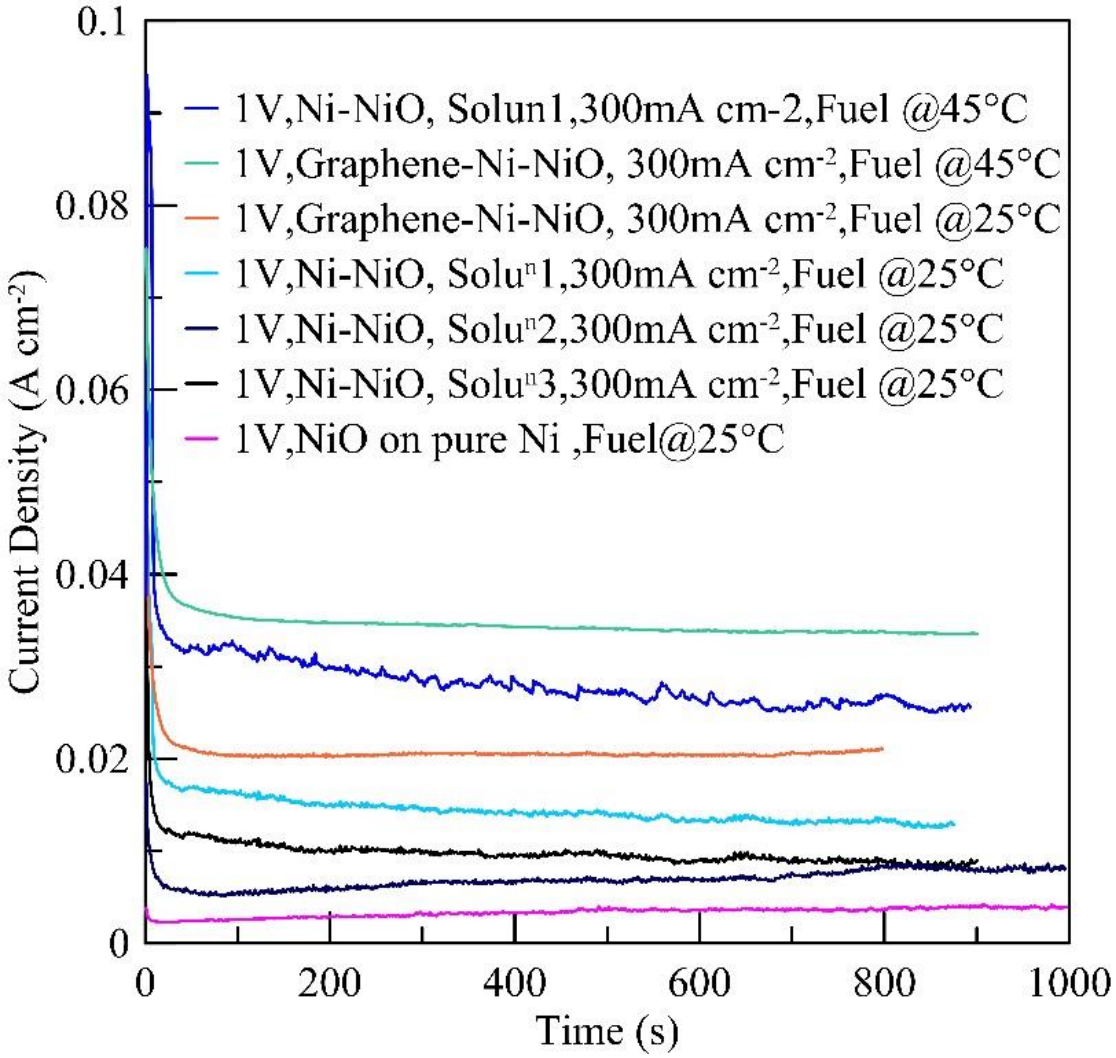

Fig.4.2c: CV of Ni-NiO and Graphene-Ni-NiO deposited at constant current density 300mA cm^{-2} at constant temperature of 60ºC, tested in 25°C and 45°C Fuel solution

4.3 Potentiodyamic Polarization (PD):

Potentiodynamic Polarization test of the electrodes was performed as per procedure described in chapter 3 under electrochemical characterization techniques. The test data is presented here in Fig 4.3a and Fig.4.3b. From the test data Reversible cell Potential and Reversible cell current on no load was calculated

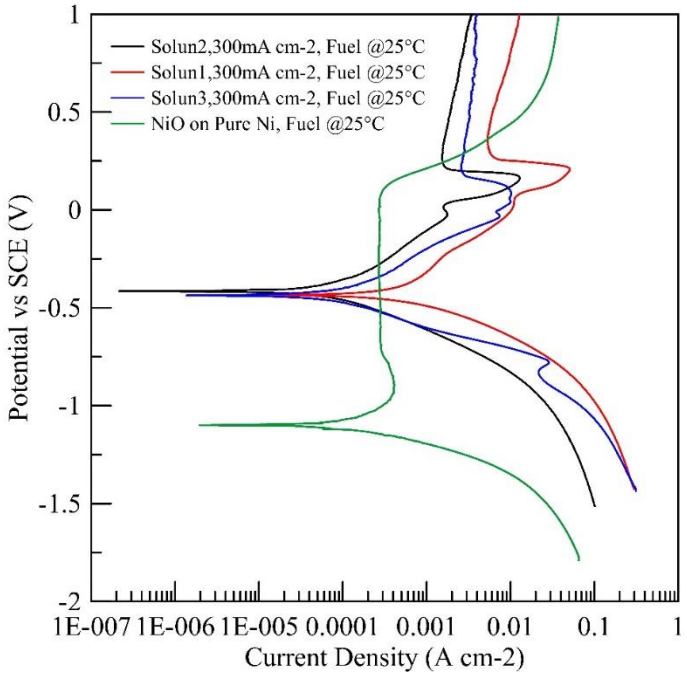

Fig.4.3a: PD of Ni-NiO deposited at constant current density 300mA cm^{-2} in varying solution chemistry at constant temperature of 60ºC

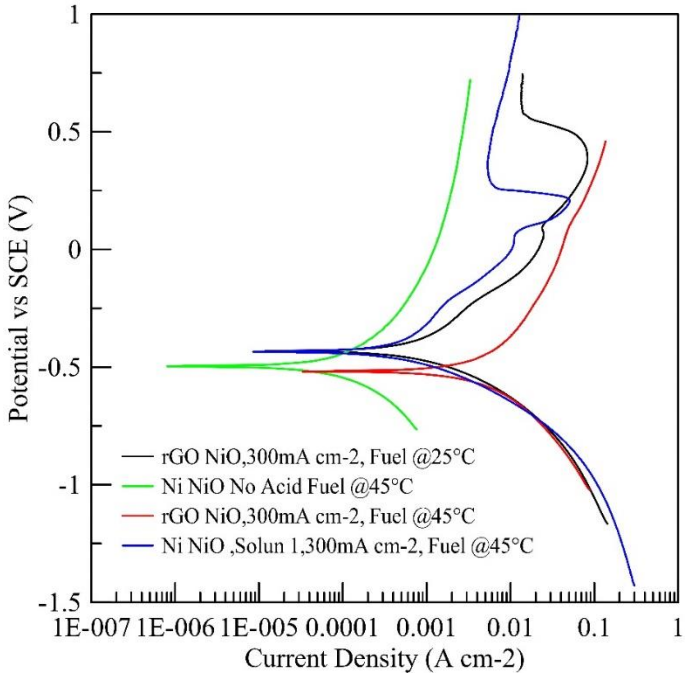

Fig.4.3b: Effect of Fuel temperature and conductivity on PD of Ni-NiO and Graphene-Ni-NiO deposited at constant current density 300mA cm^{-2} in fixed solution chemistry at constant temperature of 60ºC

4.4 Electrochemical Impedance Spectroscopy (EIS):

The Electrochemical phenomenon occurring at metal electrolyte interface can be represented by R-L-C circuit. And studied by EIS for better understanding of fundamental aspect of oxidation of the fuel on the electrolyte surface. In general, the interface consists of layer of positive charge and layer of Negative charge which is called electrical double layer which produce a capacitance (C_{dl}) or pseudo-capacitance(Y_0). In addition, there are resistive loads like polarization Resistance (R_P), solution Resistance (R_S). There may also be induction or more capacitance due to coating. The phenomenon can be interpreted Nyquist & Bode plots which are depicted and discussed in the following sections for various electro-coated catalytic electrodes.

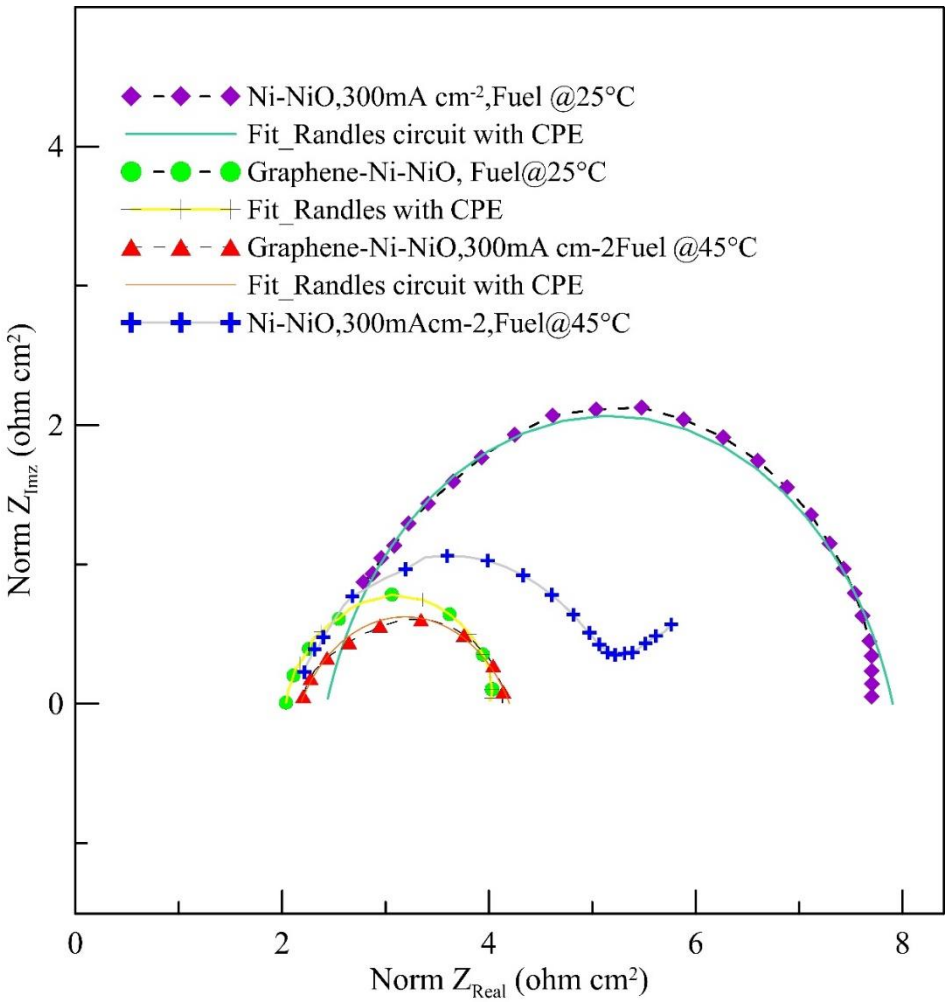

Fig.4.4a: Nyquist Plot: showing the effect of fuel temperature and addition of graphene on Ni-NiO

Fig 4.4a shows the Nyquist plot of the coated electrode at different current density. In general Nyquist curve consists of a semicircle for a pure Randle circuit. The diameter of the semicircle represents polarization resistance Rp. The model for capacitance with Warburges Resistance shows a 45degree linear line.

It is seen the diameter of the Nyquist plot semicircle changes with different current density synthesized electrodes. The most inner semicircle corresponds to 300mA/cm^2 electrode with Ni-NiO-Graphene.

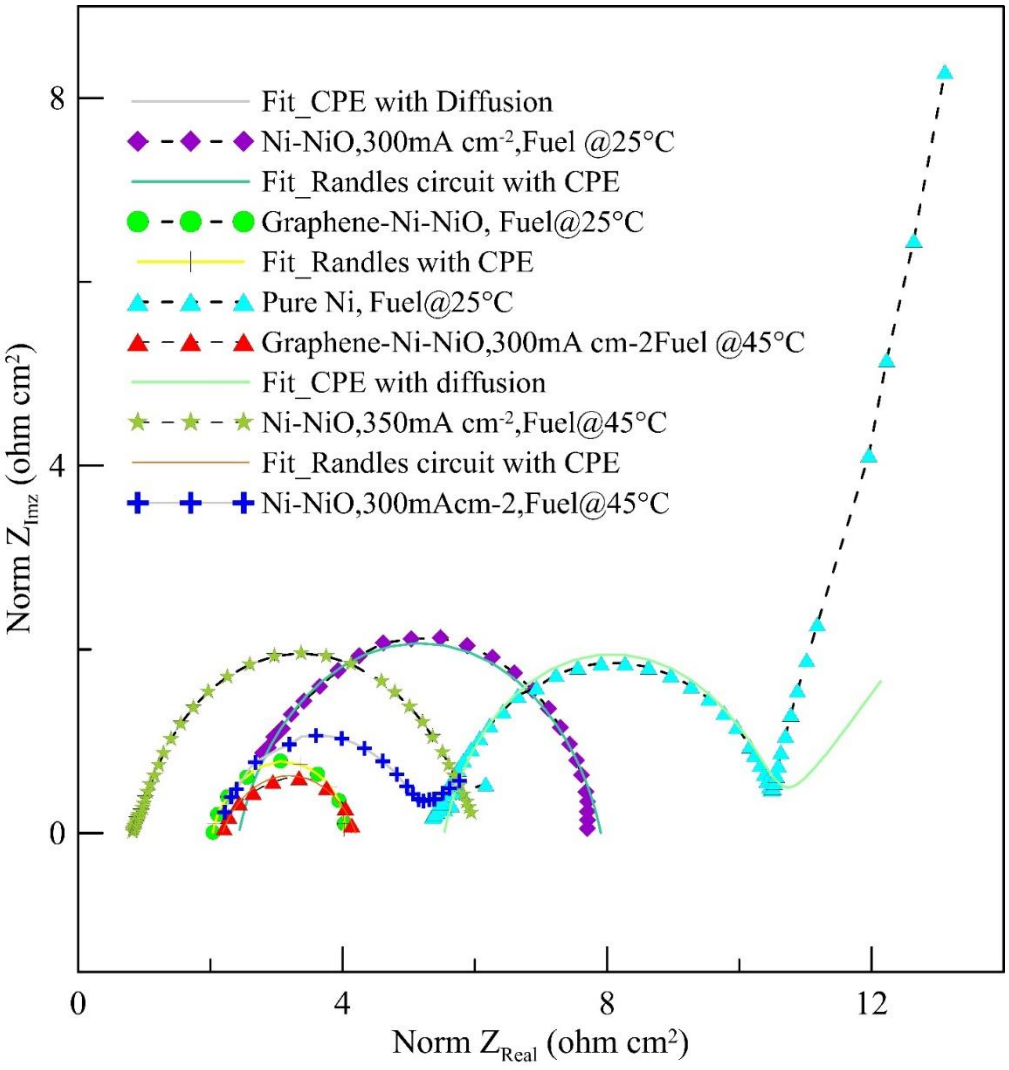

Fig.4.4b Nyquist Plot: showing the effect of fuel temperature and addition of graphene on Ni-NiO

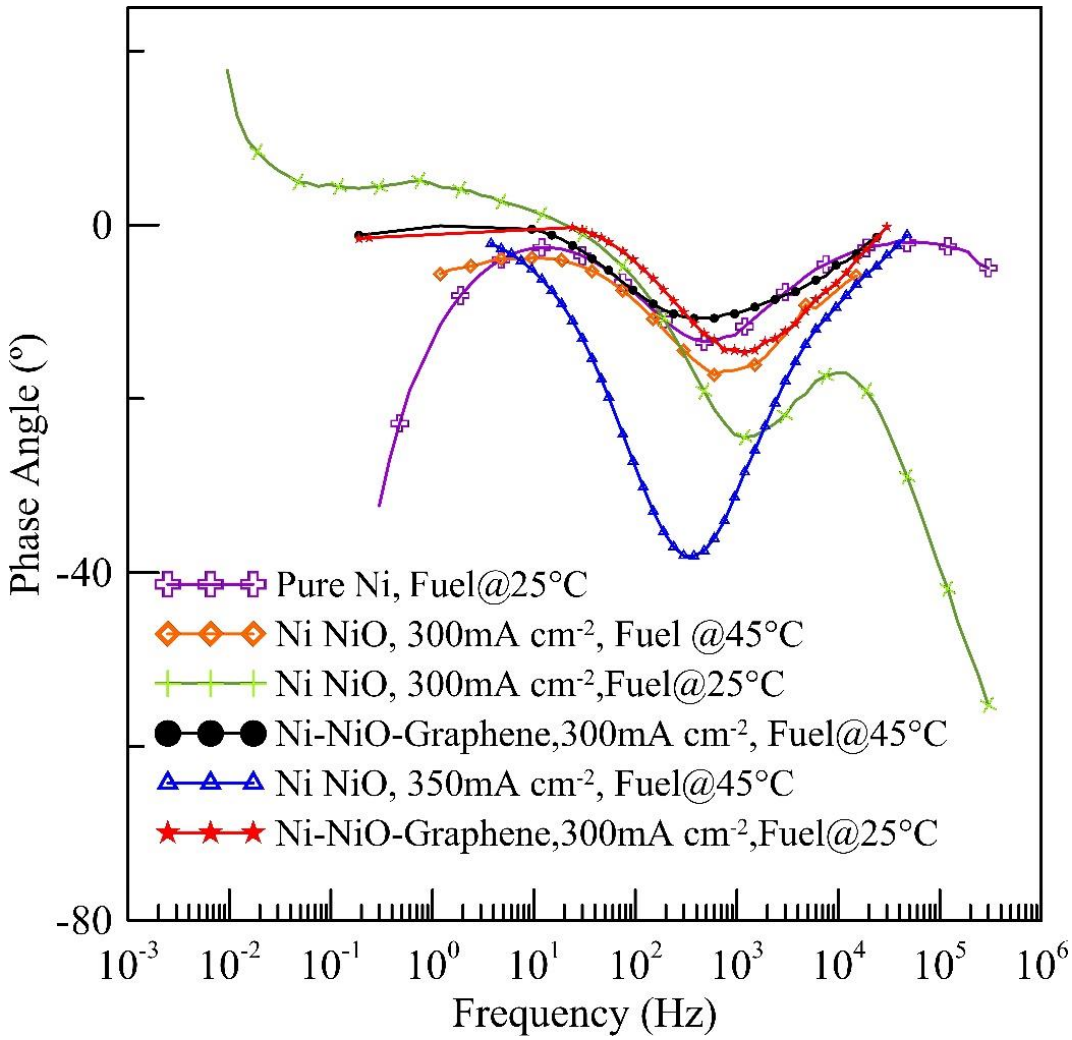

Fig.4.4c: Bode Plot (Phase Angle): showing the effect of fuel temperature and addition of graphene on Ni-NiO

It is seen that the least semicircle diameter material is matching with the highest current density material showing in CV diagram (Fig 4.1f) and CA diagram (Fig 4.2b) under section The EIS data by Bode Plot is shown in Fig.4.4b and Fig.4.4c .Bode plots indicates two parameters impedance and phase angle shift. Presence of capacitive load produce a angle shift towards -90degree.If phase angle shift is less than 90 degree. Then it is a pseudo capacitance. It behaves like a capacitive load but it is not pure capacitance.

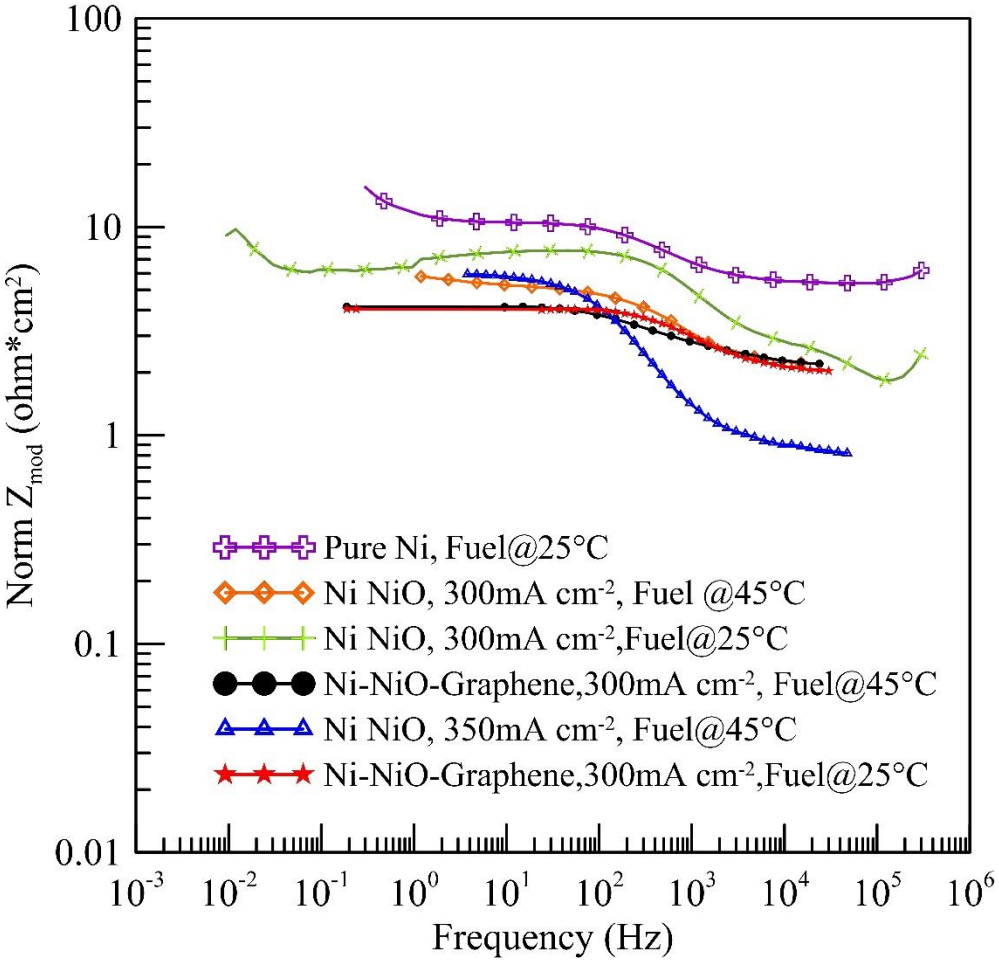

Fig.4.4d: Bode Plot (Impedance Modulus): showing the effect of fuel temperature and addition of graphene on Ni-NiO

If more than one capacitive load is present the Number of Semicircle is Nyquist plot will be twice or thrice and charge of phase angle also will be twice and thrice.

The model circuit was matched by EIS data are illustrated in Fig4.4b,. Fig4.4cand Fig4.4d. The computed EIS data obtained from Gamry Echem Analyst are tabulated in Table No 4.4e.

Material	Deposition Rate	Fuel temp	Ru(ohms*cm^2)	Rp(ohms*cm^2)	Y0(S*s^a/cm^2)	alpha	Wd(S*s^(1/2)/cm^2)	Goodness of Fit
Ni NiO	300mA cm-2	45°C	2.08	3.2	8.82E-04	7.46E-01	2.06	5.50E-04
Ni NiO	300mA cm-2	25°C	2.432	5.474	1.76E-04	8.24E-01		1.64E-04
Ni NiO Graphene	300mA cm-2	45°C	2.18	2.02	2.07E-03	7.05E-01		1.55E-04
Ni NiO	350mA cm-2	45°C	8.50E-01	5.15	8.82E-04	8.21E-01		2.21E-04
Ni NiO Graphene	300mA cm-2	25°C	2.035	2.05	4.25E-04	8.28E-01		1.18E-04

Table.4.4e: Table of values of equivalent circuit elements for corresponding EIS spectrum fitting with goodness of fit : showing the effect of fuel temperature and addition of graphene on Ni-NiO

It is seen from the table that addition of graphene decreases the Rp value of the electrode element in solution making it more active material than just Ni-NiO.

4.5.Material Characterization:

Having synthesized a good electrolytic energy material. It is now required to investigate the different phases & compounds of the coated materials XRD and 3-D morphology of the structure under Scanning Electron Microscopy.

4.5.1 X-Ray Diffraction (XRD):

To find out the phases present the XRD of the developed electrodes was performed and the results are presented below

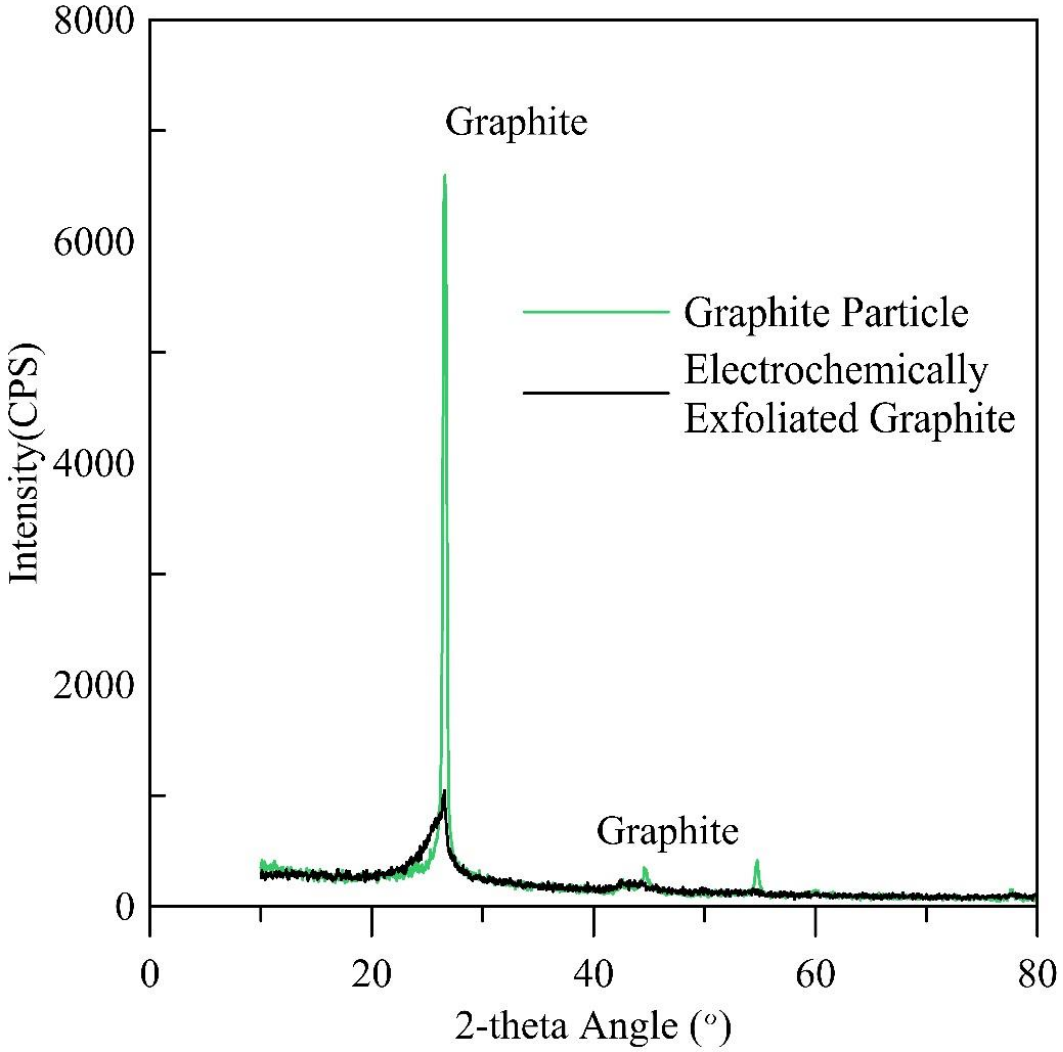

Fig.4.5.1a: XRD Pattern obtained from Untreated Graphite and electrochemically exfoliated graphite.

XRD of the above diagram shows that the electrochemically exfoliated graphite shows a flat peak on the at same 2Theta angle as graphite. This means it approaches nano scale form.

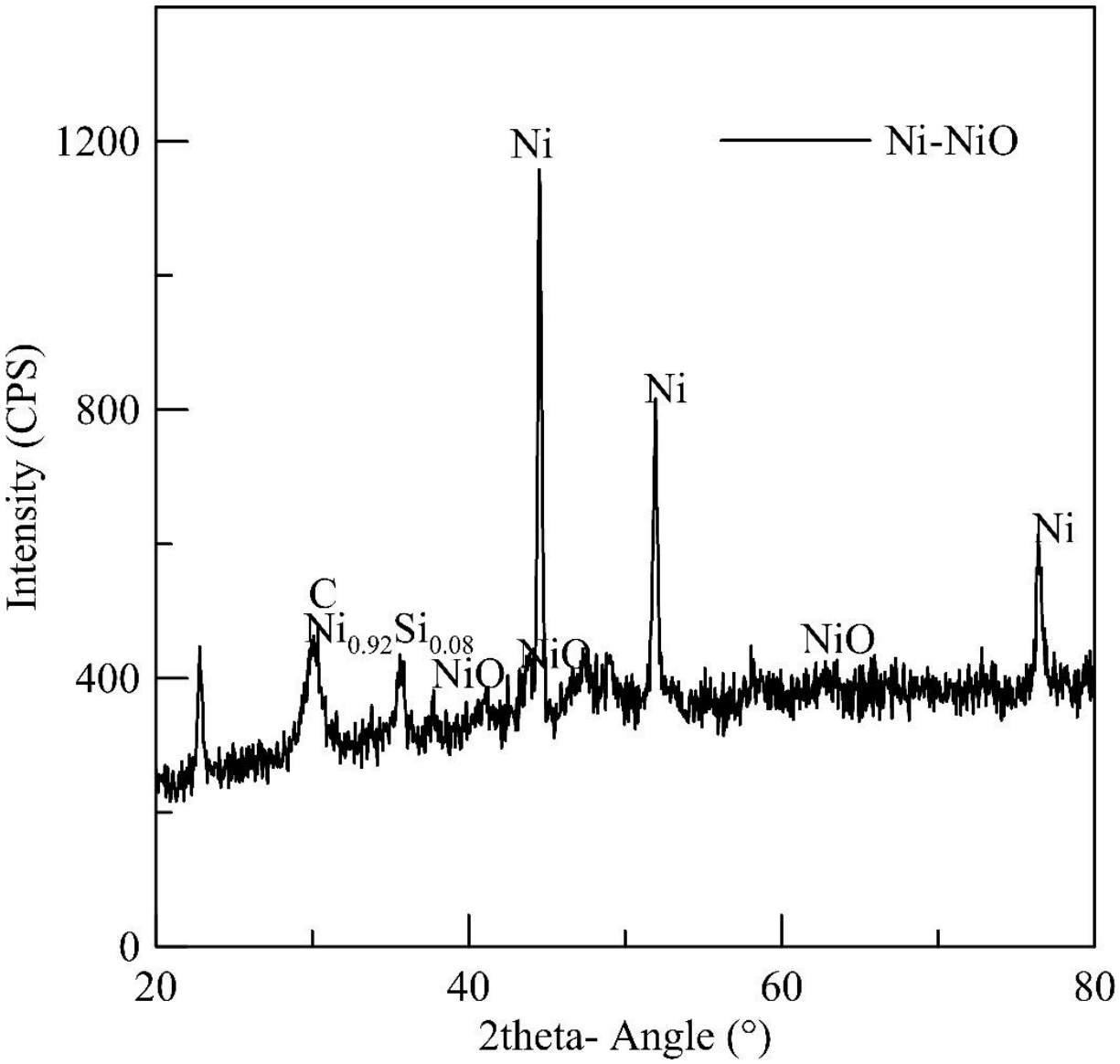

Fig.4.5.1b: XRD Pattern obtained from Ni-NiO-C

.

Fig.4.5.1b. shows the XRD of this coated material synthesized. t shows the presence of Ni, NiO, C & clearly reveals the peaks in the respective 2theta angles.So it supports the fact that the high current obtained by the material due to the presence of this Ni-NiO-C.

4

.5.2 Scanning Electron Microscopy (SEM):

To find out the morphology the SEM was carried out of the electrode surface. The results are presented below:

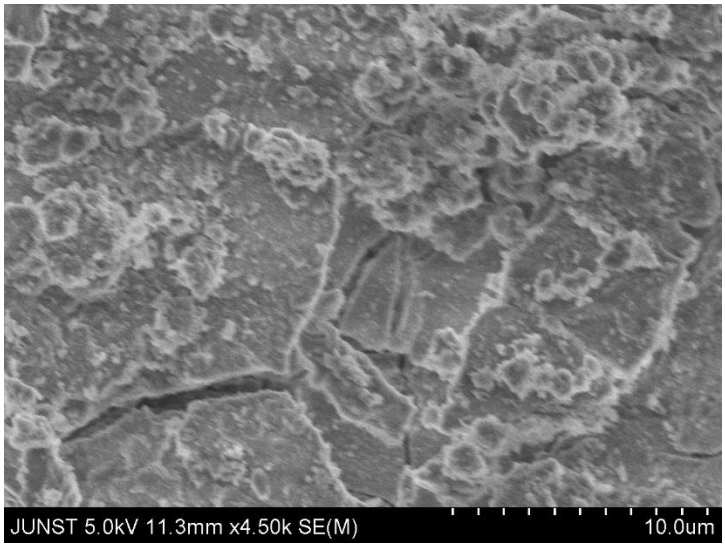

Fig4.5.2a SEM of Ni-NiO-C sample at 4500X

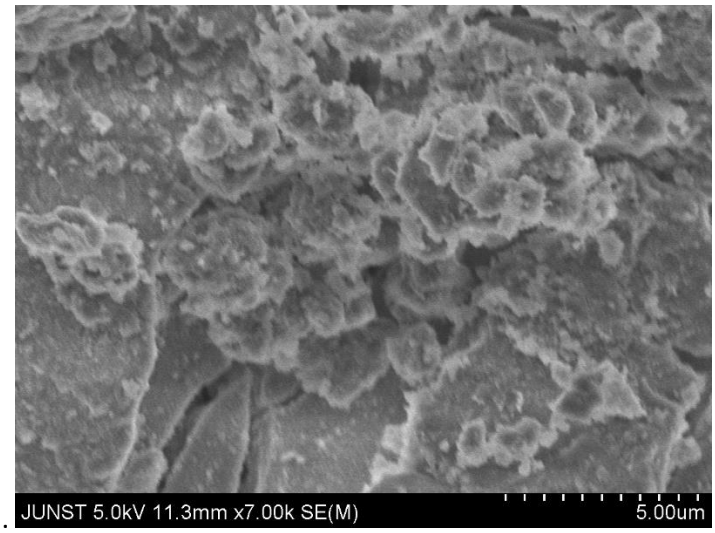

Fig4.5.2b SEM of Ni-NiO-C sample at 7000X

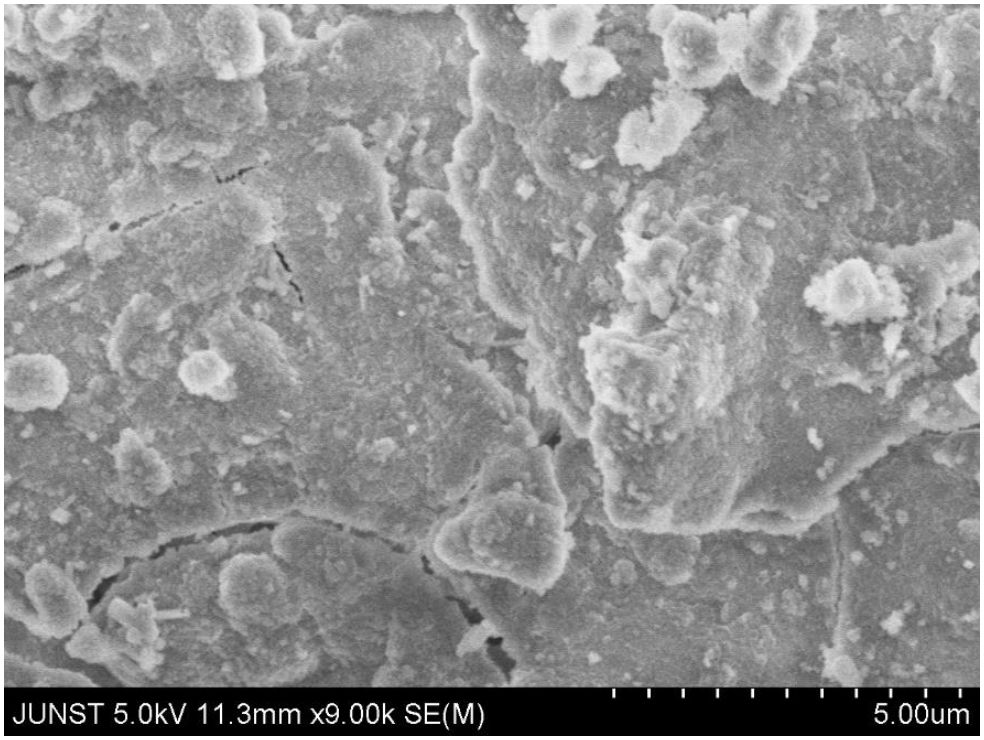

Fig4.5.2c SEM of Ni-NiO-C sample at 9000X

The morphological image analysis of the coated surface is observed under SEM show 3D microscopic structure with high surface to volume ratio. The image supports much higher 3D electrocatalytic surface area available for electro-chemical oxidation of fuel which produces high current as obtained in electro-chemical characterisation.

Chapter 5: Conclusion

Chapter 5 : Conclusion

The results and discussions in the foregoing chapters can be concluded in the following statements.

1. Ni and NiO behave as very good electro catalytic material for energy synthesis upon electro oxidation of glucose. Addition of Graphene to Ni enhances the electrocatalytic activity of the anode.
2. Electrochemical characterization by CV, CA, PD studies show high reversible cell current and cell potential.
3. Lower polarization resistance and higher capacitive impedance obtained in EIS studies support the high current density and energy produced by the material developed for electro oxidation of glucose to energy. The investigation also confirmed the addition of graphene addition is beneficial.
4. The XRD studies display the presence of Ni,NiO, C phases which are responsible for high current density for electro oxidation.
5. The morphpological image analysis of the coated surface is observed under SEM show 3D microscopic structure with high surface to volume ratio. The image supports much higher 3D electrocatalytic surface area available for electro-chemical oxidation of fuel which produces high current as obtained in electro-chemical characterisation.
6. Sugarcane solution or glucose based waste are cheap and excessively grow on our country. It is interesting to find from the present investigation that a new technology of producing energy at a economically viable rate is possible using glucose based solution over Ni and NiO electrodes

Chapter 6: Bibliography

Chapter 6: Bibliography

[1] Paul, S., & Ghosh, A. (2015). Electrochemical characterization of MnO_2 as electrocatalytic energy material for fuel cell electrode. *Journal of Fuel Chemistry and Technology*, *43*(3), 344-351.

[2] Paul, S., Naimuddin, S., & Ghosh, A. (2014). Electrochemical characterization of Ni-Co and Ni-Co-Fe for oxidation of methyl alcohol fuel with high energetic catalytic surface. *Journal of Fuel Chemistry and Technology*, *42*(1), 87-95.

[3] Bajpai, R., Roy, S., Kumar, P., Bajpai, P., Kulshrestha, N., Rafiee, J., & Misra, D. S. (2011). Graphene supported platinum nanoparticle counter-electrode for enhanced performance of dye-sensitized solar cells. *ACS applied materials & interfaces*, *3*(10), 3884-3889.

[4] Guo, S., Wen, D., Zhai, Y., Dong, S., & Wang, E. (2010). Platinum nanoparticle ensemble-on-graphene hybrid nanosheet: one-pot, rapid synthesis, and used as new electrode material for electrochemical sensing.*ACS nano*,*4*(7), 3959-3968.

[5] Li, W. Y., Xu, L. N., & Chen, J. (2005). Co_3O_4 nanomaterials in lithium-ion batteries and gas sensors. *Advanced Functional Materials*, *15*(5), 851-857.

[6] Han, S., Yun, Y., Park, K. W., Sung, Y. E., & Hyeon, T. (2003). Simple Solid-Phase Synthesis of Hollow Graphitic Nanoparticles and their Application to Direct Methanol Fuel Cell Electrodes. *Advanced Materials*, *15*(22), 1922-1925.

[7] Li, G. R., Xu, H., Lu, X. F., Feng, J. X., Tong, Y. X., & Su, C. Y. (2013). Electrochemical synthesis of nanostructured materials for electrochemical energy conversion and storage. *Nanoscale*, *5*(10), 4056-4069.

[8] Zhu, Y., Murali, S., Cai, W., Li, X., Suk, J. W., Potts, J. R., & Ruoff, R. S. (2010). Graphene and graphene oxide: synthesis, properties, and applications. *Advanced materials*, *22*(35), 3906-3924.

[9] You, T., Niwa, O., Tomita, M., & Hirono, S. (2003). Characterization of platinum nanoparticle-embedded carbon film electrode and its detection of hydrogen peroxide. *Analytical chemistry*, *75*(9), 2080-2085.

[10] Tang, H., Chen, J., Yao, S., Nie, L., Deng, G., & Kuang, Y. (2004). Amperometric glucose biosensor based on adsorption of glucose oxidase at platinum nanoparticle-modified carbon nanotube electrode. *Analytical Biochemistry*, *331*(1), 89-97.

[11] O'Mahony, A. M., & Wang, J. (2013). Nanomaterial-based electrochemical detection of explosives: a review of recent developments. *Analytical Methods*, *5*(17), 4296-4309.

[12] Zhu, J., Lu, Z., Aruna, S. T., Aurbach, D., & Gedanken, A. (2000). Sonochemical synthesis of SnO_2 nanoparticles and their preliminary study as Li insertion electrodes. *Chemistry of Materials*, *12*(9), 2557-2566.

[13] Yao, J., Shen, X., Wang, B., Liu, H., & Wang, G. (2009). In situ chemical synthesis of SnO_2–graphene nanocomposite as anode materials for lithium-ion batteries. *Electrochemistry communications*, *11*(10), 1849-1852.

[14] Leech, D., Kavanagh, P., & Schuhmann, W. (2012). Enzymatic fuel cells: Recent progress. *Electrochimica Acta*, *84*, 223-234.

[15] Nørskov, J. K., Rossmeisl, J., Logadottir, A., Lindqvist, L. R. K. J., Kitchin, J. R., Bligaard, T., & Jonsson, H. (2004). Origin of the overpotential for oxygen reduction at a fuel-cell cathode. *The Journal of Physical Chemistry B*, *108*(46), 17886-17892.

[16] Paul, S. (2015). Nanomaterials synthesis by electrodeposition techniques for high-energetic electrodes in fuel cell. *Nanomaterials and Energy*, *4*(1), 80-89.

[17] Wang, Y., Liu, J., Liu, L., & Sun, D. D. (2011). High-quality reduced graphene oxide-nanocrystalline platinum hybrid materials prepared by simultaneous co-reduction of graphene oxide and chloroplatinic acid. *Nanoscale research letters*, *6*(1), 241.

[18] Chaudhuri, S. K., & Lovley, D. R. (2003). Electricity generation by direct oxidation of glucose in mediatorless microbial fuel cells. *Nature biotechnology*, *21*(10), 1229.

[19] Murray, E. P., Tsai, T., & Barnett, S. A. (1999). A direct-methane fuel cell with a ceria-based anode. *Nature*, *400*(6745), 649.

[20] Park, S., Vohs, J. M., & Gorte, R. J. (2000). Direct oxidation of hydrocarbons in a solid-oxide fuel cell. *Nature*, *404*(6775), 265.

[21] Rapoport, B. I., Kedzierski, J. T., & Sarpeshkar, R. (2012). A glucose fuel cell for implantable brain–machine interfaces. *PloS one*, *7*(6), e38436.

[22] Oncescu, V., & Erickson, D. (2013). High volumetric power density, non-enzymatic, glucose fuel cells. *Scientific reports*, *3*, 1226.

[23] Zebda, A., Cosnier, S., Alcaraz, J. P., Holzinger, M., Le Goff, A., Gondran, C., ... & Cinquin, P. (2013). Single glucose biofuel cells implanted in rats power electronic devices. *Scientific reports*, *3*, 1516.

[24] Pakapongpan, S., Tuantranont, A., & Poo-arporn, R. P. (2017). Magnetic Nanoparticle-Reduced Graphene Oxide Nanocomposite as a Novel Bioelectrode for Mediatorless-Membraneless Glucose Enzymatic Biofuel Cells. *Scientific reports*, *7*(1), 12882.

[25] Wu, H., Wang, J., Kang, X., Wang, C., Wang, D., Liu, J., ... & Lin, Y. (2009). Glucose biosensor based on immobilization of glucose oxidase in platinum nanoparticles/graphene/chitosan nanocomposite film. *Talanta*, *80*(1), 403-406.

[26] Minteer, S. D., Atanassov, P., Luckarift, H. R., & Johnson, G. R. (2012). New materials for biological fuel cells. *Materials Today*, *15*(4), 166-173.

[27] Luo, J., Wang, L., Mott, D., Njoki, P. N., Lin, Y., He, T., ... & Zhong, C. J. (2008). Core/shell nanoparticles as electrocatalysts for fuel cell reactions. *Advanced Materials*, *20*(22), 4342-4347.

[28] Bing, Y., Liu, H., Zhang, L., Ghosh, D., & Zhang, J. (2010). Nanostructured Pt-alloy electrocatalysts for PEM fuel cell oxygen reduction reaction. *Chemical Society Reviews*, *39*(6), 2184-2202.

[29] Wanjala, B. N., Luo, J., Loukrakpam, R., Fang, B., Mott, D., Njoki, P. N., ... & Malis, O. (2010). Nanoscale Alloying, Phase-Segregation, and Core− Shell Evolution of Gold− Platinum Nanoparticles and Their Electrocatalytic Effect on Oxygen Reduction Reaction. *Chemistry of Materials*, *22*(14), 4282-4294.

[30] Luo, J., Njoki, P. N., Lin, Y., Wang, L., & Zhong, C. J. (2006). Activity-composition correlation of AuPt alloy nanoparticle catalysts in electrocatalytic reduction of oxygen. *Electrochemistry communications*, *8*(4), 581-587.

[31] Li, Y., Lu, A., Ding, H., Jin, S., Yan, Y., Wang, C., ... & Wang, X. (2009). Cr (VI) reduction at rutile-catalyzed cathode in microbial fuel cells. *Electrochemistry Communications*, *11*(7), 1496-1499.

[32] Zhang, Z., Xin, L., Sun, K., & Li, W. (2011). Pd–Ni electrocatalysts for efficient ethanol oxidation reaction in alkaline electrolyte. *International Journal of Hydrogen Energy*, *36*(20), 12686-12697.

[33] Das, D., Sen, P. K., & Das, K. (2008). Mechanism of potentiostatic deposition of MnO2 and electrochemical characteristics of the deposit in relation to carbohydrate oxidation. *Electrochimica Acta*, *54*(2), 289-295.

[34] Hu, Y., Zhang, H., Wu, P., Zhang, H., Zhou, B., & Cai, C. (2011). Bimetallic Pt–Au nanocatalysts electrochemically deposited on graphene and their electrocatalytic characteristics towards oxygen reduction and methanol oxidation. *Physical Chemistry Chemical Physics*, *13*(9), 4083-4094.

[35] Kumar, K. S., Haridoss, P., & Seshadri, S. K. (2008). Synthesis and characterization of electrodeposited Ni–Pd alloy electrodes for methanol oxidation. *Surface and Coatings Technology*, *202*(9), 1764-177

[36] Guchhait, S. K., & Paul, S. (2015). Synthesis and characterization of ZnO-Al_2O_3 oxides as energetic electro-catalytic material for glucose fuel cell. Journal of Fuel Chemistry and Technology, 43(8), 1004-1010.